Chem Soc Rev

Phosphorus Promotion and Poisoning in Zeolite-based Materials: Synthesis, Characterisation and Catalysis

Journal:	*Chemical Society Reviews*
Manuscript ID:	CS-REV-02-2015-000109.R2
Article Type:	Review Article
Date Submitted by the Author:	10-May-2015
Complete List of Authors:	Van der Bij, Hendrik; Debye Institute for Nanomaterials Science, Inorganic Chemistry and Catalysis, Utrecht University Weckhuysen, Bert; Debye Institute for Nanomaterials Science, Inorganic Chemistry and Catalysis Group, Utrecht University

Chem Soc Rev

RSCPublishing

REVIEW ARTICLE

Phosphorus Promotion and Poisoning in Zeolite-based Materials: Synthesis, Characterisation and Catalysis

Cite this: DOI: 10.1039/x0xx00000x

Hendrik E. van der Bij,[a] and Bert M. Weckhuysen*[a]

Received 00th January 2012,
Accepted 00th January 2012

DOI: 10.1039/x0xx00000x

www.rsc.org/

Phosphorus and microporous aluminosilicates, better known as zeolites, have a unique, but poorly understood relationship. For example, the phosphatation of the industrially important zeolite H-ZSM-5 is a well-known, relatively inexpensive and seemingly straightforward post-synthesis modification applied by chemical industry, not only to alter its hydrothermal stability and acidity, but also to increase e.g. selectivity towards light olefins in hydrocarbon catalysis. On the other hand, phosphorus poisoning of zeolite-based catalysts, used for $DeNO_x$ of exhaust fuels, poses a problem for their use in diesel engine catalysts. Despite the wide impact of phosphorus-zeolite chemistry, the exact physicochemical processes that take place require a more profound understanding. This review article provides the reader with a comprehensive and state of the art overview of the academic literature, from the first reports in the late 1970s until the most recent studies. In the first part an in-depth analysis is made, which will reveal universal physicochemical and structural effects of phosphorus-zeolite chemistry on the framework structure, accessibility, and strength of acid sites. The second part discusses the hydrothermal stability of zeolites and clarifies the promotional role that phosphorus plays. The third part of the review paper links the structural and physicochemical effects of phosphorus on zeolite materials with catalytic performance in a variety of catalytic processes, including alkylation of aromatics, catalytic cracking, methanol-to-hydrocarbon processing, bio alcohol dehydration, and ammonia selective catalytic reduction (SCR) of NO_x. Based on these insights we discuss potential applications and important directions for further research.

1. Introduction

Biomass conversion, crude-oil cracking, automotive catalysis and gas-to-liquid technology [1-4] are just a few of the many chemical processes where zeolites are used, or have the potential to be used as catalysts. Made from the abundant elements silicon, aluminium and oxygen, they are relatively cheap and environmentally friendly materials. In the expected transitional period where the global economy will move from fossil-based to truly sustainable resources, zeolites still have an important part to play. Therefore, it is paramount to understand the chemistry of these fascinating shape-selective 'micron-scale molecule making factories' on a fundamental level, from macro-scale to nano-scale. Insights in their morphology, accessibility, active sites, selectivity, stability and deactivation behaviour will allow us to further improve and extend their use as valuable catalyst materials.

A seminal example of a zeolite material – and one very relevant for this review – is zeolite H-ZSM-5. Figure 1 shows H-ZSM-5 at different dimension scales. Single H-ZSM-5 crystals are often coffin- or parallelepiped-shaped and can have sizes ranging from 100 nm to 100 μm.[5-7] Inside the crystal we find a three-dimensional microporous channel system, as can be seen in Figure 1b and 1c, which act as transport channels for molecules. The channel system comprises of straight and sinusoidal pores. Both pore types run parallel to the [010] and [100] crystallographic planes, respectively. As the two pore types are connected at regular intersections, molecules can diffuse into the [001] direction as well. The average pore size of these channels is around 5.5 x 5.5 Å.[8] At the positions where the microporous channels intersect, cavities form of 6.36 Å in diameter.[9] Consequently, molecules that exceed the dimensions of the channels are prohibited from entering or exiting the zeolite. However larger molecules can form in the cavities at the channel intersections. These shape-selective properties

make H-ZSM-5 and zeolites in general effectively act as molecular sieves.

The channel system of H-ZSM-5 stems from the well-ordered MFI-type framework. All zeolite frameworks consist of silica and alumina tetrahedra, which are linked by shared oxygen atoms. The solid-acid character of zeolites follows from the negatively charged AlO_4^- tetrahedra that are incorporated into the zeolite lattice. Each of such tetrahedra leads to a net negative charge on the framework, which needs to be compensated by a counter-cation. If these counter-cations are protons, strong Brønsted acid sites are formed, as shown in Figure 1e. More aluminium substituted in the framework leads to more acid sites. Therefore, the framework silicon to aluminium ratio is an important parameter for zeolites and is generally written as Si/Al ratio. The combined shape selectivity and strong acidity of zeolites create the desired properties for, e.g. catalytic hydrocarbon cracking.

Although the bulk of zeolites are used as hydrocarbon cracking or isomerisation catalysts in oil refining processes, zeolites are also used in many other catalytic processes, including the alkylation of aromatics with oxygenates, (bio) alcohol conversion to light olefins, dewaxing of hydrocarbons, aromatics and fuels, the dehydrogenation of paraffins, dehydration of (bio-) alcohols, and in photocatalytic reactions. [10-26] It is therefore that zeolites are not just catalysts for present day oil refining purposes, but also important catalysts for future green/clean hydrocarbon production processes.

In the late 1970s it was found that post-modification with a phosphorus precursor can change the acidic and shape selective properties of zeolites. [10, 27-30]. The most notable phosphorus-containing precursor is H_3PO_4, which is added to the zeolite by wet impregnation. After this step the zeolite is thermally treated in air/oxygen, a process better known as calcination, which decomposes the phosphorus precursors into (poly-)phosphates and phosphorus pentoxides. It has been found that phosphorus can act to zeolites either as a promoter, e.g., in the Fluid Catalytic Cracking (FCC) process and the Methanol-To-Hydrocarbons (MTH) reaction, or as a poison in Ammonia Selective Catalytic Reduction (NH_3-SCR) of exhaust gasses, i.e. NOx. [27, 31, 32]

As a promoter, phosphorus is well known to improve the hydrothermal stability of zeolite H-ZSM-5. [33, 34] At the same time phosphorus interacts with the acid sites of zeolites, leading to a reduction in acid site number and strength. [35] Furthermore, if phosphorus is located in the micropores of zeolites, it can either favourably alter its shape selective effects, or block micropores and reduce the overall accessibility of the zeolite material. [36] While the presence of phosphorus can be beneficial, for example in the MTH reaction where it boosts light olefin selectivity and especially towards propylene, [31] it is deleterious for NH_3-SCR DeNOx applications. [37]

The promotional effects of phosphorus are well-known to the refining industry, which follows from the numerous patents including all major refining companies. [23, 38-49] Not surprisingly, many academic groups have reported on the effects of phosphorus on zeolites. However, the exact nature of phosphorus-zeolite interaction has always been a point of discussion, which makes phosphorus-zeolite chemistry an important topic from a fundamental perspective as well. Many models for possible interactions have been proposed over the years and the main division of opinion lies between the question whether permanent phosphorus-framework interaction exists or not. [34, 50-56]

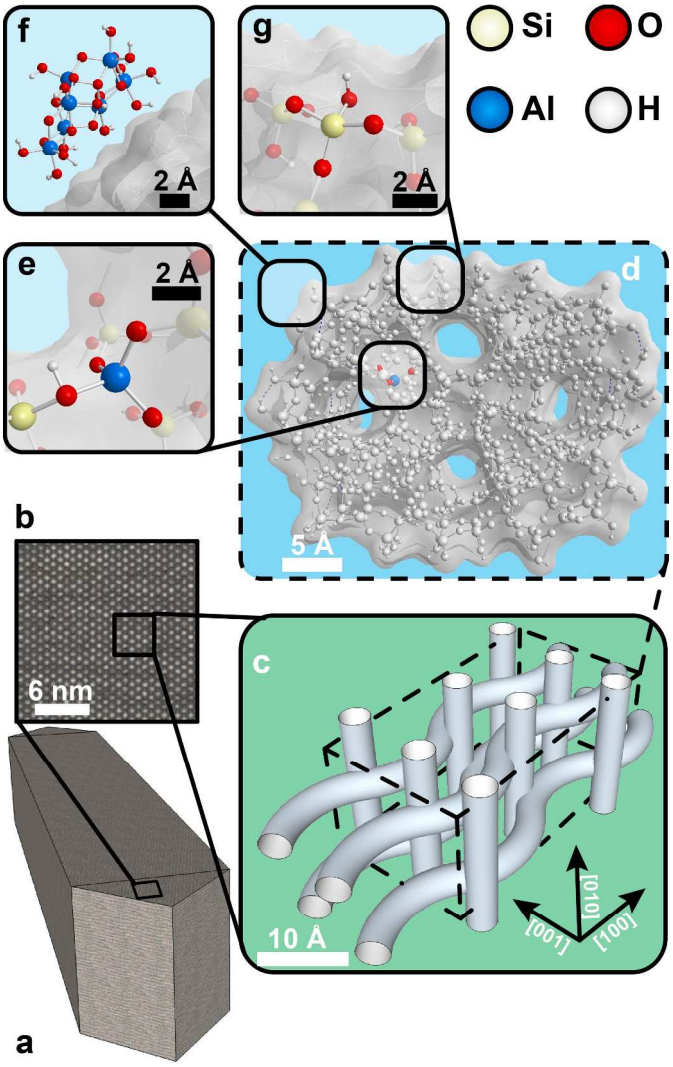

Fig. 1 Overview of zeolite H-ZSM-5 at different dimension scales. a) A micron-sized coffin shaped H-ZSM-5 crystal. b) Closer inspection of the [001][100] plane, revealing the straight pores. c) The three dimensional channel system of H-ZSM-5 consists of intersecting straight and sinusoidal pores. d) The channel system follows from the MFI-framework, which comprises of linked silica and alumina tetrahedra. e) A tetrahedrally coordinated framework aluminium (TFAl) atom leads to a net negative charge on the framework. In H-ZSM-5 this negative charge is compensated by a proton, which leads to a Brønsted acid site. The OH group in SiOHAl is generally referred to as a bridging hydroxyl group. f) Dealumination leads to the formation of extra-framework aluminium, here shown as boehmite. g) terminal silicon and aluminium atoms, which are generally found on the zeolite external surface form silanol and aluminol groups.

In the case of permanent phosphorus-framework interaction the most intuitive explanation would be the incorporation of

phosphorus into the zeolitic framework. Examples of these suggestions are shown in Scheme 1 a-d. These interactions can be subsequently categorized in (a-b) phosphorus bonded to the bridging oxygen group of Si-O-Al, [52, 57] (c) Si-O-P bonds, [35] and (d) Al-O-P bonds.[55, 58] Other possible phosphorus-framework interactions have been suggested to be reversible, as shown in Scheme 1 e-f. [34, 50, 59] Examples of suggestions for reversible interactions are (e) intramolecular bonds, [59] or (f) protonation of phosphoric acid by zeolitic bridging hydroxyl groups.[34] It has also been proposed that (g) phosphorus does not interact at all with the zeolite framework and phosphorus only interacts with extra-framework aluminium. [56]

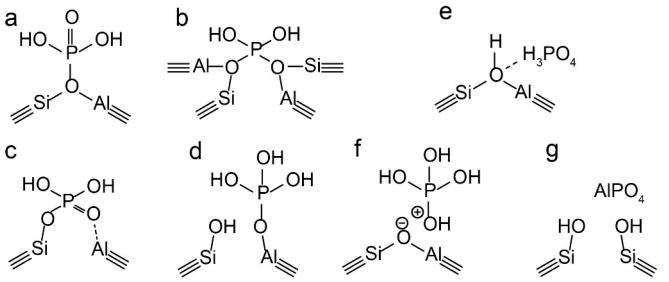

Scheme 1. Suggestions from the literature for phosphorus-framework interactions. (a-c and f) are most cited. (a) Kaeding et al., [52] (b) Xue et al., [57] (c) Lercher et al., [35] (d) Zhuang et al., [58] (e) Abubakar et al. [59] (f) Blasco et al., [34] and (g) Caro et al. [56]

We believe the topic of phosphorus-zeolite chemistry will become increasingly important since (i) hydrothermal stabilisation of zeolites is paramount for the industrial application of zeolites as catalysts to produce hydrocarbons. Especially in regeneration after coke deactivation, (bio) alcohol conversion and dehydration, the presence and formation of water, combined with high temperatures lead to permanent deactivation of the zeolite catalysts. [60-62] (ii) There is an ever-increasing demand for propylene and selective production by phosphated zeolites is a serious candidate for selective large-scale production. [31, 63, 64] (iii) The relative high phosphorus content in biofuel poses a challenge for zeolites as NH_3-SCR catalysts. [65]

Elucidation of the nature of phosphorus-zeolite chemistry is expected to reveal the reasons behind hydrothermal stabilisation, acid site alteration and changes in catalytic performance. This Review Article provides the reader with a thorough analysis of the academic literature on phosphorus-zeolite chemistry, which has, to our best knowledge, never been the subject of a review paper. The goal of this Review Article is to find structural and physicochemical trends in phosphorus modified zeolites. Subsequently, we aim to link these structural properties to the catalytic poisoning and promotional effects found in catalysis. The Review Article ends with an outlook on future research directions.

2. Methods of Phosphorus Introduction

When considering the vast literature on zeolites modified by phosphorus, it is clear that the use of incipient wetness impregnation (IWI) or wet impregnation (WI) is the most practiced phosphatation method. [31, 33, 34, 50, 51, 53, 57-60, 63, 64, 66-85] The precursor of choice is phosphoric acid. [10, 31, 33, 34, 50, 51, 53, 55, 58, 63, 64, 66-68, 70, 71, 73, 75, 77, 78, 81-87] Less acidic precursors such as $NH_4H_2PO_4$ [34, 36, 88, 89] and $(NH_4)_2HPO_4$ [57, 60, 69, 74, 76, 79, 80, 86] are used as well. After impregnation, the materials obtained are first dried at temperatures ranging from 70 °C to 120 °C, sometimes at reduced pressures. Afterwards samples are calcined at elevated temperatures ranging from 450 °C to 650 °C for durations ranging from 1 h to 6 h.

Another preparation method is quite similar to impregnation, with the difference that the sample is mixed under reflux conditions with an aqueous solution of H_3PO_4, where the concentration of H_3PO_4 corresponds to the desirable phosphorus content. Water is removed by evaporation at reduced pressures. Subsequently, the samples are dried and calcined. [35, 54, 56, 86, 87, 90-92]

Besides phosphoric acid and ammonium phosphates, different precursors are used as well. Especially popular in the 1980s was the use of trimethylphosphite (TMPT). This precursor was solved in *n*-octane and mixed with a zeolite slurry. The mixture was stirred under reflux conditions, then filtered, washed with e.g. n-pentane and dried at 120 °C. Subsequently, the sample was calcined at elevated temperatures.[29, 52, 54, 90, 93, 94] Gas-phase deposition is also a technique used to transfer a phosphorus precursor into a H-ZSM-5 zeolite. Precursors reported with this technique are trimethylphosphite (TMPT)[78, 94, 95], triphenylphosphine (TPP)[96, 97], trimethylphosphine (TMP)[54, 59, 90-92] and phosphorus pentachloride (PCl_5).[98] The zeolite was contacted with the vapour phase of these precursors at elevated temperatures ranging from 360 °C to 600 °C. In the case of TMP a cycle was repeated a couple of times.

Different precursors used in combination with impregnation methods are diphenylphosphinous (DPP) acid, TPP and phosphorus trichloride (PCl_3), dissolved in methylene chloride, carbon tetrachloride and benzene, respectively.[17] However, it is important to understand that all these methods are followed by a post-calcination, which renders the phosphorus precursors into phosphates.

Finally it has been tried to incorporate phosphorus into the MFI framework by synthesizing ZSM-5 with a phosphorus precursor in the reaction gel.[99, 100] Gao et al. used a phosphatation method which was coined as the hydrothermal dispersion method. Here H-ZSM-5 is mixed with $(NH_4)_2HPO_4$ and reacted at 140 °C and at 0.3 MPa for 2 h.[101, 102]

Even though there are many different ways to introduce phosphorus, it can be read in the following sections that the overall physicochemical effects on the zeolite structure are very similar. Nevertheless, significant differences that arise due to the method of phosphorus introduction will be highlighted when applicable.

3. Physicochemical Changes

3.1 Physical and Chemical Phosphorus-Framework Interactions

In the following section we will describe three distinct phases that can be found in phosphated zeolites, which consist of (i) a separate phosphate and zeolite phase (ii) a phosphate-zeolite interface phase and (iii) a separate aluminium-phosphate and zeolite phase. The formation of these phases depends strongly on the pre- and post-treatment of the zeolite during phosphorus introduction. However, it is important to understand that these phases often exist simultaneously in phosphated zeolites.

3.1.1 Separate Phosphate and Zeolite Phases. As was mentioned in the previous section, the phosphatation method of choice is the introduction of phosphoric acid to a zeolite by means of wet impregnation. Several characterization methods have indicated that this method leads to a higher concentration of phosphorus species on the zeolite surface compared to phosphorus in the zeolite bulk. [29, 37, 51, 86, 87, 96] Most of these species are monomeric phosphates and di- or polyphosphates.[56] Generally, smaller phosphate chains are found before calcination of the zeolite, while larger condensed polyphosphate species and phosphorus pentoxides form after heat treatment due to dehydration [59, 86] Rehydration hydrolyses phosphorus pentoxide species into smaller mono-, di-, and small polyphosphate chains. [56, 59] Lischke and co-workers showed that smaller phosphates could easily be removed by elution with hot water. However, the condensed polyphosphates that form after thermal treatments prove more difficult to remove by washing with hot water. [36, 50, 55, 67, 85, 86] The majority of these phosphorus species have no interaction with the zeolite phase and thus the phosphate and zeolite phase can be considered separate. Nevertheless, the phosphate species have an influence on zeolite accessibility as will be discussed in section 3.2.

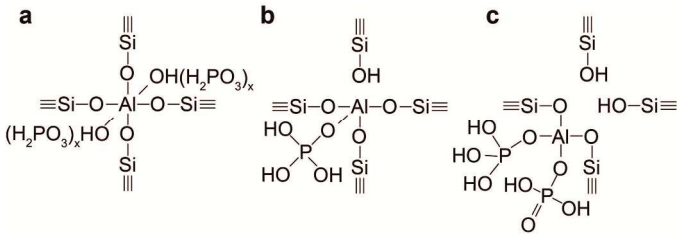

Scheme 2. Suggestions of different phosphorus-zeolite interface phases found in phosphated and thermally treated H-ZSM-5. (a) TFAl forced into a six-fold coordination by physically bonded phosphate species (b) Local SAPO interface (c) Local SAPO interface with aluminium connected to two phosphates.[55, 58, 71, 86]

3.1.2 Phosphorus-Aluminium Attraction: Reversible Interfaces. As phosphorus is found dominantly on the zeolite surface as a separate phosphate phase, only a relative small amount of phosphorus enters the pores of the zeolite. However, with increasing phosphorus loadings more phosphorus moves into the channel system. [33, 34, 53, 56, 58, 71, 77, 81, 84, 86, 87] There, phosphate species can form reversible and irreversible interfaces with framework aluminium. It has been shown that phosphoric acid can coordinate with tetrahedrally coordinated zeolite framework aluminium (TFAl), inducing an octahedral coordination on aluminium. [69] This change from four-fold to six-fold coordination is fully reversible, as washing with hot water removes phosphorus and reverts the six-coordinated aluminium back to classic TFAl atoms. [50, 86] Increasing phosphorus loadings leads to an increased formation of these interactions, as more phosphorus enters the zeolite pores. [103] After thermal treatment of the phosphated zeolite, these interactions remain reversible. [50, 85, 86, 103] Suggestions for the nature of these reversible interactions are TFAl atoms that are physically coordinated by phosphate species [86], or ionic bonding [34, 103] and a postulated structure is shown in Scheme 2 a.

Besides a change in aluminium coordination, the presence of phosphoric acid can distort the electronic environment of TFAl atoms, which has been suggested to arise from hydrogen bonding between the hydrogen atoms in H_3PO_4 and framework oxygen and/or Brønsted acid sites and phosphate oxygen groups. [59, 86, 104] Also this type of interaction has been found to be fully reversible.[86]

Both interaction types lead to an observable decrease in TFAl species and a reduction in Brønsted acid sites, as we will discuss in the following sections. [30, 50, 86, 103] Permanent damage to the framework before thermal treatment of phosphated zeolites has not been reported for the MFI topology. However, as we will read in section 3.1.4, other topologies appear to suffer framework damage after phosphorus introduction. [30]

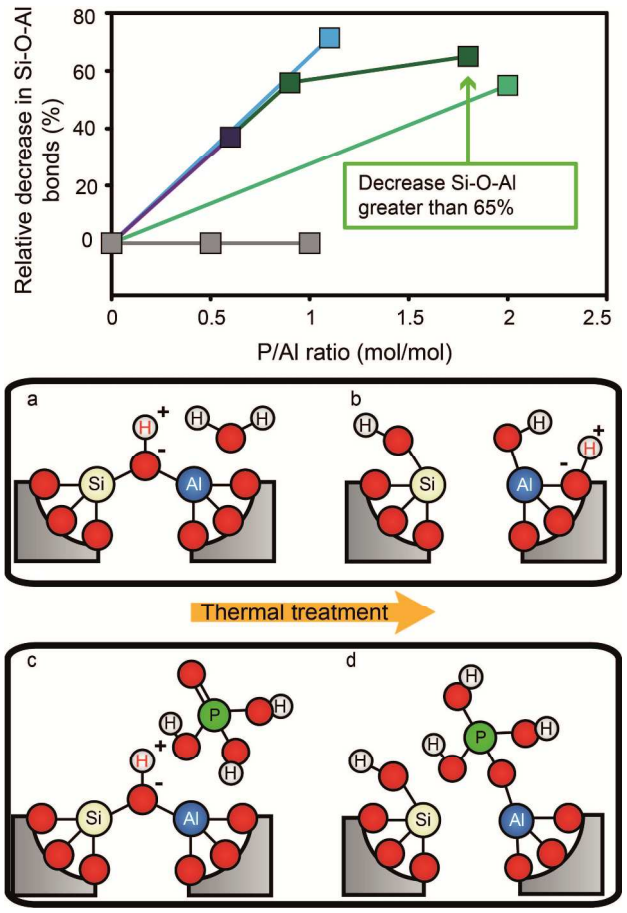

Fig. 2 The decrease in Si-O-Al bonds vs. P/Al ratio after phosphatation. Values are calculated from reported Si/Al ratios obtained by ^{29}Si MAS NMR. ■ = Caro et al.[56] ■ = Zhuang et al.[58] ■ = Abubakar et al.[59] ■ = Blasco et al.[34] ■ = Li et al.[82] The decrease in TFAl for P/Al ratio 1.8 corresponds to a reported Si/Al ratio greater than 200, so the actual percentage is higher. (a-d) Postulated mechanism of "SAPO-fication" by Si-O-Al bond hydrolysis during thermal treatment in the presence of H_2O and H_3PO_4. [55, 58, 60, 86, 103, 105, 106]

3.1.3. *Phosphorus-Aluminium Attraction: Permanent Interfaces and SAPO-fication.* During a thermal treatment, high temperatures and the presence of H_2O in the atmosphere will lead to the hydrolysis of Si-O-Al bonds (Figure 2 a-b) . [107] In the presence of phosphorus even more Si-O-Al bonds are hydrolysed. [56, 58, 59, 82, 87] This effect can be observed in Figure 2, where the decrease in the percentage of Si-O-Al bonds is plotted against the P/Al ratios in phosphated and thermally treated zeolites. The figure indicates a trend that depends on P/Al ratio, which suggests phosphorus species actively promote the hydrolysis of Si-O-Al bonds during thermal treatment. With high phosphorus loadings above 2.5 wt.%, internal silanol groups at defect sites have been reported to form. [53, 64, 94, 108] The exception is the work of Blasco et al. where no dealumination is observed. In the respective work, the post calcination of the sample was mild (500 °C, 1 h), which could have been insufficient for the cleaving of Si-O-Al bonds. The decrease in Si-O-Al bonds goes hand in hand with a decrease in classic TFAl atoms. [33, 34, 37, 50, 53, 55-59, 69, 71, 77, 78, 81, 82, 84-87, 92, 98, 103, 109-112]

Due to the decrease in Si-O-Al bonds, the crystallinity of zeolites can be reduced to a small extent after introduction of phosphorus and subsequential thermal treatment, but the framework structure is maintained and no additional crystalline phases have been reported. [30, 53, 58, 63, 64, 71, 73, 76, 77, 81-84, 101, 111] Loss in crystallinity was found for samples treated with acidic and non-acidic precursors and with different acidities used in the impregnation solution, excluding acid leaching as the source of crystallinity loss.

After thermal treatment of phosphated H-ZSM-5, H-ITQ-13, and H-MCM-22 a new type of aluminium is formed at the cost of classic TFAl atoms. [33, 34, 57, 58, 71, 75, 82, 85-87, 92, 103, 111, 113]. In other zeolite topologies these species are not observed. [30, 37, 109] This new type of aluminium can attributed mostly to four-coordinated, but also to five-, and six-, coordinated aluminium species still present at lattice positions in a highly distorted environment, due to chemical and spatial interactions with phosphate species. [55, 58, 71, 86, 103] It is suggested that phosphate species bond with terminal Si-O-Al-OH groups of partially dislodged TFAl species that form during thermal treatment (Figure 2 b), effectively leading to the formation of local silico-aluminophosphate (SAPO) interfaces (Shown in Figure 2 c-d). [58, 71, 86] It is expected that the positively charged $[PO_4]^+$ unit in the SAPO interface balances the negative charge on the zeolite framework. ^{27}Al-^{31}P INEPT-HETCOR NMR experiments have confirmed that these species have Al-O-P bonds. [55]

During this "SAPO-fication" process the zeolite material sees a gradual increase of this new SAPO interface phase with increasing phosphorus loadings. [34, 53, 71, 82, 92, 103, 108] Still, a maximum amount of SAPO interfaces has been observed. [71, 103, 108] Local SAPO interfaces do not disappear after washing with hot water. [85, 86, 103] However, washing with NH_4F did remove the species. [34]

Importantly, Damodaran and co-workers have shown that local SAPO interfaces are not a single defined species, but consist of a variety of framework aluminium and phosphorus interactions, e.g. phosphate mono- and bi-dentate ligands on four-, five-, and six-coordinated aluminium atoms, of which a few are shown in Scheme 2 b-c.[55, 71] With higher phosphorus loadings the spectroscopic signatures for phosphorus in local SAPO interfaces become more $AlPO_4$-like. [55, 114] This indicates that more Si-O-Al bonds are broken and replaced with Al-O-P bonds with increasing phosphorus content. [55, 58, 114] The afore-mentioned increase in Si-OH groups with increased P content agrees with this model. [53, 64, 94, 108] Neither different pH values nor phosphorus precursors seem to have an influence on the appearance of local SAPO interfaces after thermal treatment. [34, 78, 86] The SAPO-fication model has also been proposed in environmental and soil science studies, where aluminium impregnated mesoporous silicates are effective absorbers of phosphates from the environment, as phosphates are suggested to form Si-O-Al-O-P(HO_3) monolayers. [115]

All the findings described in this section indicate an attraction between phosphorus and framework aluminium.

Furthermore, there is a synergistic effect between the presence of phosphorus and subsequent heat treatment, as phosphorus actively promotes the dealumination of zeolites during thermal treatment, indicating that the formation of Al-O-P bonds is energetically favoured.

Although in the last ten years more indirect evidence for framework connected Si-O-Al-O-P(HO_3)-R species has been reported, the existence of SAPO interfaces has not yet been directly proven. [55, 58, 71, 86, 103, 108] In order to clearly establish bonding between the phosphorus with framework aluminum we suggest the addition of *J*-coupling $^{27}Al - {}^{29}Si$ correlation NMR spectroscopy [116] in combination with *J*-coupling ^{27}Al- ^{31}P correlation NMR spectroscopy. [55]

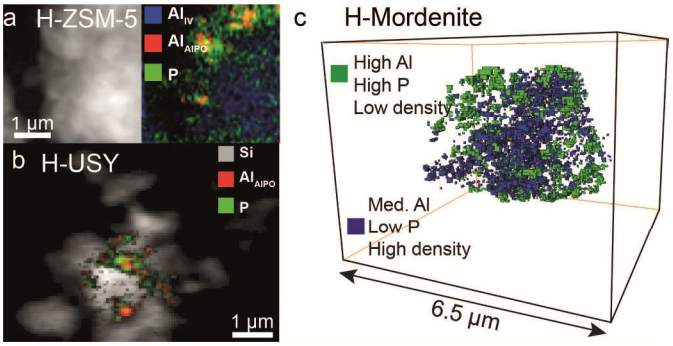

Fig. 3 X-ray absorption microscopy results show $AlPO_4$ 'islands' in phosphated (a) H-ZSM-5, (b) H-USY and (c) H-mordenite. Adapted from references [87, 114]

3.1.4 Aluminium-Phosphate Formation. The attraction between phosphates and aluminium is even stronger when aluminium is present as extra-framework aluminium (EFAl) in zeolites. Phosphoric acid will readily react with any extra-framework aluminium species present in zeolites. [28, 30, 50, 58, 87, 98, 114, 117] Several spectroscopic techniques have shown that EFAl species disappear when phosphorus is introduced to zeolites. [28, 34, 50, 64, 70, 87, 92, 114] It has been established that extra-framework AlO(OH) species that are present before phosphatation will react with phosphorus and form an extra-framework amorphous $AlPO_4$ phase. [28, 50, 87, 114, 117] This amorphous $AlPO_4$ phase is heterogeneously distributed and mostly found on the external surface of zeolites, as shown in Figure 3. d[28, 114] Thermal treatment leads to the crystallisation of the phase as α-cristoballite/trydimite $AlPO_4$ islands. [28, 30, 87, 114] It has not been found that the $AlPO_4$ phase migrates during thermal crystallisation. [114]

In the case of the zeolites mordenite, ZSM-11, MCM-22 and Y the treatment with a phosphate precursor does not only lead to the reaction of phosphoric acid with extra-framework aluminium. Framework aluminium is leached from the lattice by phosphorus and amorphous $AlPO_4$ is formed. [30, 82, 98, 109, 113, 114, 117] The tendency of framework aluminium to be leached out from the lattice by acid treatment depends on the topology of the zeolite. [118] In the case USY, which has a high aluminium content in its framework, the extraction of framework aluminium leads to a collapse of the structure. [114] In the case of zeolite mordenite almost all TFAl atoms are leached out of the framework, while the overall framework remains intact. [114] Although the effect of topology on lattice aluminium extraction by phosphorus would benefit from further systematic study, the findings exemplify the attraction between phosphorus and aluminium.

3.1.5 Phosphorus Framework Incorporation? In the previous sections we have read that it is the phosphorus-aluminium interaction that drives physicochemical changes in zeolites. However, especially in early literature, it is has been suggested that phosphorus is incorporated into the zeolite framework. This is understandable, as it would be the most intuitive explanation for the observed changes in zeolites upon phosphatation. However, in order for phosphorus to be incorporated into the framework, stable Si-O-P bonds need to be formed. In contrast, many theoretical works have shown that Si-O-P bonds are very unstable. [119-123] However, in one theoretical study it was suggested that the substitution of penta-coordinated phosphorus into the framework is possible at high temperatures. [110] Yet experimentally, the work of Barrer and co-workers has shown that attempts to substitute phosphorus for silicon and aluminium in silicates and aluminosilicates only leads to the formation of $AlPO_4$ and silica. [124]

In a frequently cited study by Xue et al., it was proposed that phosphorus is incorporated in vacant framework positions in dealuminated H-ZSM-5, for which convincing spectroscopic evidence was given. (See Scheme 1 b).[57] However, a detailed study on the formation of phoshosilicate glasses shows that the spectroscopic signatures Xue and co-workers attributed to Si-O-P species in fact stem from polyphosphate species that are trapped in a siloxane (or silica) framework and do not have any interaction with silicon species through bond. [125] In this work, it was convincingly argued that P-OH and Si-OH groups rather self-condense than form cross-links. [125] The only Si-O-P bonds in phosphosilicate glasses that have been unequivocally assigned by means of *J*-coupling NMR spectroscopy have NMR resonances, which to our best knowledge, have never been reported in phosphated zeolite literature. [126]

Therefore, due to unstable character of Si-O-P bonds compared to the stable character of Al-O-P bonds and the lack of any experimental evidence, [127] it seems very implausible that Si-O-P bonds easily form in phosphated zeolites and complete framework incorporation by phosphorus is thus very unlikely.

3.2 Changes in Porosity, Accessibility and Acidity Induced by Phosphorus

In the previous section we discussed what type of phases and interactions can be found in phosphated zeolites. The following section will discuss the effect of these phases and interactions on the zeolite porosity, accessibility and acidity.

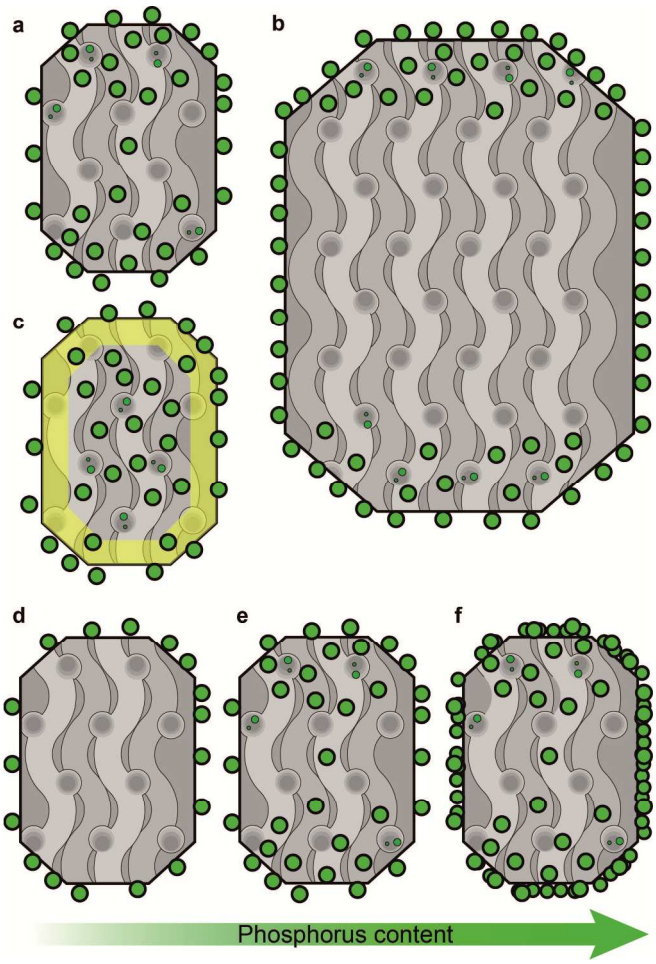

Fig. 4 Proposed schematic model of phosphorus species location depending on crystal size, aluminium distribution and increasing phosphorus weight loadings. The model is based on XPS data by references [29, 51, 96] ^{129}Xe NMR and 1H NMR tracer desorption by references [56, 69] and STXM studies [86, 87] a) Typical distribution of phosphorus on H-ZSM-5. b) Effect of crystal size. c) Effect of aluminium distribution. Yellow is an aluminium-poor region. d-f) Effect of increasing phosphorus loading. Due to diffusion limitations the location of phosphorus is more dependent on actual P weight loading than P/Al ratio. Crystals are viewed along the [100][001] plane.

3.2.1 Location and Distribution of Phosphorus. As was mentioned before, several characterization methods have shown that there is a higher concentration of phosphorus species on the zeolite surface compared to phosphorus in the zeolite bulk. [29, 37, 51, 86, 87, 96] The method of phosphorus introduction seems to play an important role in the distribution of phosphorus. It has been reported that by using the hydrothermal dispersion method to introduce phosphorus, mentioned in section 2, a more homogeneous distribution throughout the micropore channel system can be obtained, while impregnation lead to a high concentration of phosphorus species on the surface. [101, 102]

While most of the phosphate species present on the external surface have no interaction with the zeolite phase, it has been shown that the presence of phosphorus on the external surface of a zeolite goes hand in hand with a decrease or disappearance of surface hydroxyl groups after phosphatation. [54, 56, 69, 72-74, 86, 87, 92, 94] In line with the presence of a phosphorus distribution gradient, is that at low loadings, below 2 wt.% P, the amount of surface hydroxyl groups decreases faster than those found in the bulk. Only when the surface is covered with surfactant do phosphorus species enter the zeolite bulk immediately at low loadings, shown in Figure 4 d. [54, 56, 69, 72-74, 86, 87, 92, 94] The latter results would indicate that phosphate species first form an phosphate-zeolite interface phase with the external silanol and aluminol groups.

With increasing crystal size the ratio of $P_{Surface}/P_{Bulk}$ species increased (Figure 4 b). [51] This suggests that phosphorus species experience diffusion limitations. Interestingly, when the concentration of aluminium was higher in the zeolite bulk than the external surface, the distribution of phosphorus was homogeneous (Figure 4 c).[29] This latter finding is in line with the previously described attraction between framework aluminium and phosphorus.

When phosphorus loadings are increased, the phosphorus species tend to move further into the zeolite, as it was found that all aluminium species and corresponding acid sites are affected by the presence of phosphorus (Figure 4 e).[33, 34, 53, 56, 58, 71, 77, 81, 84, 86, 87] However, with progressively increasing phosphorus loadings, the concentration of phosphorus surface species increases faster than those in the bulk and after phosphorus loadings exceed 5 wt.% mostly excess phosphorus is deposited on the external surface.[35, 37, 53, 55, 56, 69, 78, 81] Platelets of excess polyphosphates have found to be present on the outer surface. [35] A schematic drawing of this effect is presented in Figure 4 f. Evidence for the aggregation of zeolite particles by phosphorus modification can be found in the literature as well and it has been suggested that phosphorus promotes the self-annealing of external Si-OH groups. [56, 87, 103]

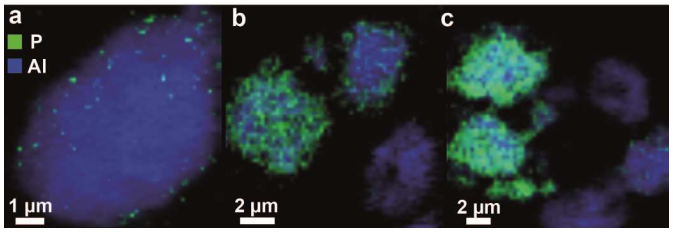

Fig. 5 X-ray absorption microscopy results from references [86, 87]. Chemical maps of zeolite H-ZSM-5 (Si/Al = 11.5) clusters are modified by wet impregnation with a phosphate precursor followed by calcination (P/Al = 0.5), constructed from aluminium K-edge spectra and phosphorus K-edge spectra stacks. Precursors used are (a-b) H_3PO_4 and (c) $(NH_4)_2HPO_4$ ■ = Al ■ = P Resolution is 60 x 60 nm.

The distribution gradient of phosphorus has recently been shown by our group in a spatially-resolved manner using X-ray absorption microscopy and representative images are shown in Figure 5. From the figure it can furthermore be observed that by introduction of phosphorus using wet impregnation, inter-particle heterogeneities in phosphorus distribution can be found. [86, 87]

Summarizing, phosphorus weight loading, P/Al ratio, surface OH groups, aluminium distribution, crystal size and the phosphorus introduction technique all play a role in the eventual distribution of phosphorus species.

3.2.2 Accessibility and Porosity. As phosphorus is present on the external surface and in the micropores, the phosphatation of zeolites leads to a decrease in micropore volume and surface area. As more phosphorus is able to penetrate the zeolite interior at higher weight loadings, the decrease is gradually more severe with increasing phosphorus content. [30, 31, 33-35, 53, 57, 64, 68, 69, 71, 73, 74, 76-79, 81-85, 87, 89, 102, 103, 108, 111, 114, 128-130]

Commonly, the decrease in micropore volume and surface area is attributed to dealumination, partial blockage of channels by phosphorus species and aggregation of zeolite particles. Chen and co-workers suggested that the presence of phosphorus changed diffusional characteristics by decreasing pore dimensions and openings, leading to longer diffusion pathways for reactants and products.[10, 17, 93] These results have been confirmed and Janardhan et al. reported that phosphorus forms monolayer islands throughout the MFI channel system. [36, 69] Adsorption with the probe molecules cyclohexane and n-heptane showed a strong decrease in accessibility for samples with more than 3 wt.% loading of phosphorus species. [68]

When a phosphate precursor is used to introduce phosphorus, most of the phosphorus is present as ortho-, pyro-, and polyphosphates before thermal treatment. [86, 103] As up to the majority of these soluble species can be removed by hot water washing before thermal treatment, the external surface area and micropore volume of phosphated zeolites can be restored to 95% of the parent material. [53] However, washing of a phosphated zeolite after thermal treatment leads only to a partial restoration of surface area and micropore volume. [36, 53, 85, 89] One of the reasons is that after thermal treatment phosphorus species become condensed and occluded and have a decreased solubility in water, while the other is the formation of a permanent phosphorus-zeolite interface phase, as discussed in section 3.1. [86, 103]

Nevertheless, it can be observed that most of the loss in micropore volume and surface area that is detectable by physisorption techniques, is caused by the presence of water soluble (poly-) phosphate species. Seo and co-workers suggested that changes in micropore volume caused by (permanent) phosphorus-framework interactions were too small to detect by conventional physisorption methods, but could be discriminated by ^{129}Xe NMR spectroscopy. [69]

3.2.3 Acid Site Loss. The solid acid sites in zeolites are the active sites in zeolite catalysis. As was discussed in the introduction, a perfect crystalline zeolite material has only three types of acid sites. The strongest acid sites are formed by the protons present in framework bridging hydroxyl groups, while the remaining acid sites are very weak and comprise of surface terminal silanol and aluminol groups. [112] Thermal treatment, applied to convert the ammonium form of zeolites into H-zeolites, can lead to dealumination.[107]

With the breaking of Si-O-Al bonds new acid sites can form. These are silanol groups that form at defect sites and extra-framework aluminium species. [112] Furthermore, framework aluminium species that are only partially connected to the framework can form Lewis or Brønsted acid sites. [86, 131, 132]

After modification of zeolites with phosphorus, followed by thermal treatment there is a gradual decrease in bridging hydroxyl groups and silanol groups, with increasing phosphorus content. [29, 31, 34-36, 50, 53, 54, 56-58, 60, 64, 66, 68-70, 72, 73, 76-79, 81-87, 89, 90, 92, 94-96, 103, 111, 113, 117, 128-130] Within a single study, as can be seen in Figure 6, the relative decrease in Brønsted acid sites correlates quite well with the P/Al ratio. [34] In the same study, it was established that all acid sites were accessible to probe molecules and that the decrease in acid site number can therefore most likely not be attributed to physical blocking of acid sites.

As all reported samples have been thermally treated after phosphatation, one obvious cause of Brønsted acid site loss is the dealumination induced by the thermal treatment. The breaking of Si-O-Al bonds and the formation of Al-OH groups have been observed after phosphatation and subsequent calcinations. [56, 58, 59, 82, 84, 86, 94, 133] Thermal treatment can attribute to at least 45% of the loss in strong acid sites. [86] Furthermore, as phosphorus promotes the hydrolysis of Si-O-Al bonds, the gradual decrease in acid sites with increasing phosphorus loadings is understandable. [56, 58, 59, 82, 87] Also, the expected formation of neutral local SAPO interfaces will decrease the overall negative charge on the zeolitic framework, reducing the amount of protons that can act as counter cations.

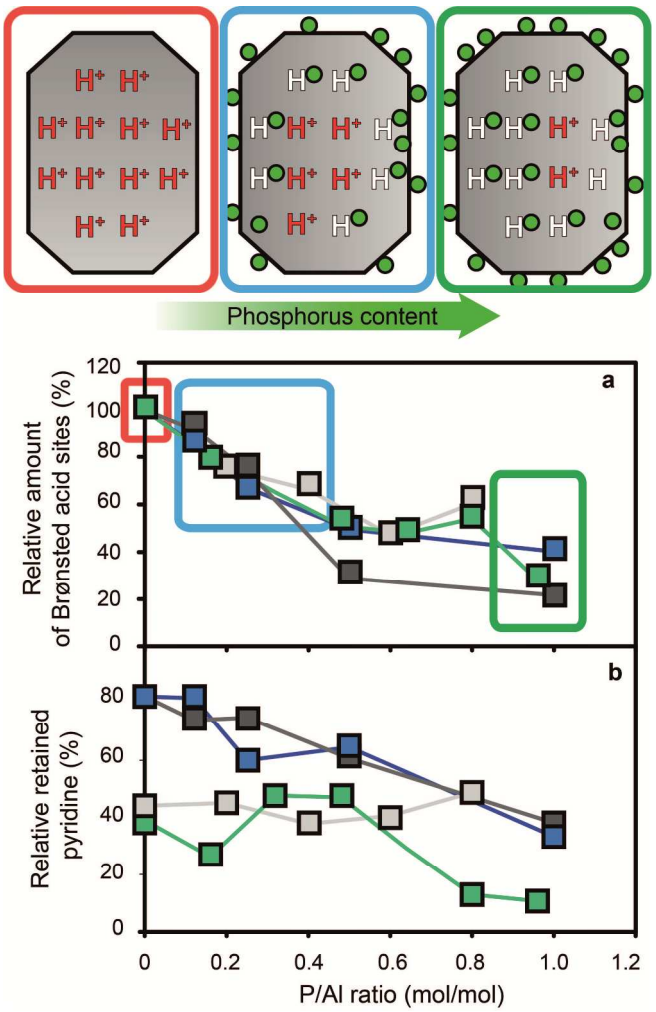

Fig. 6 a) Relative amount of Brønsted acid sites vs. P/Al ratio, as determined by pyridine adsorption at 150 °C. The concentration is relative to the parent material. b) Relative acid site strength of Brønsted acid sites vs. P/Al ratio, as determined by pyridine adsorption at 150 °C and 350 °C. The percentage is the protonated pyridinium ion concentration of a sample at 350 °C, divided by the protonated pyridinium ion concentration of the same sample at 150 °C. ■ = H-ZSM-5 + $NH_4H_2PO_4$ (Si/Al = 15) ■ = H-ZSM-5 + $NH_4H_2PO_4$ (Si/Al = 25) ■ = H-ZSM-5 + H_3PO_4 (Si/Al = 25) ■ = H-ZSM-5 + $NH_4H_2PO_4$ (Si/Al = 40). Data obtained from the work of Blasco et al. [34]

In the literature it is reported that with phosphorus weight loadings above 5 wt.% the amount of strong acid sites has almost completely disappeared. [35, 68, 77, 81] The Brønsted/Lewis acid site ratio is found to decrease in phosphorus modified samples, which would indicate that Lewis acid sites are not as much affected by phosphorus as Brønsted acid sites. [35, 64, 76, 86, 91, 96, 100, 102]

However, phosphorus introduction without any thermal treatment also leads to a decrease in strong acid sites. [50, 86, 103] This decrease is completely reversible, as washing of the sample leads to a full retrieval of all strong acid sites, without any signs of permanent dealumination. [50, 86] Furthermore, it was calculated that after thermal treatment, the number of Brønsted acid sites does not correspond to the amount of tetrahedrally coordinated framework aluminium (TFAl) species in phosphated samples. [92, 103] That is, 20% more TFAl species were present than Brønsted acid sites. When the sample was mixed with alumina or washed with hot water, these phosphorus species reacted and the 20% of Brønsted acid sites were retrieved. [92, 103] The recovery of acid sites after thermal treatment by hot water washing was confirmed in other studies. [36, 85, 86, 103]

It is important to understand from the former results that phosphorus is not only a dealuminating agent, but reduces the number of Brønsted acid sites in a reversible way. Therefore, although Si-O-Al bond breaking and the formation of local SAPO interfaces during SAPO-fication are the reasons for permanent acid site loss, reversible interactions of phosphorus with framework aluminium as described in section 3.1.2 lead to a reversible loss in acid sites as well. At this moment the exact nature of the reversible acid site loss is not well understood, but a recent computational study suggested that hydrogen bonding between orthophosphoric acid and framework oxygen could lead to the formation of a $H_3PO_4H^+$ group, similar to a suggestion of Blasco and co-workers. [34, 104] We are hopeful that future computational studies will elucidate the origin of reversible acid loss in phosphated zeolites.

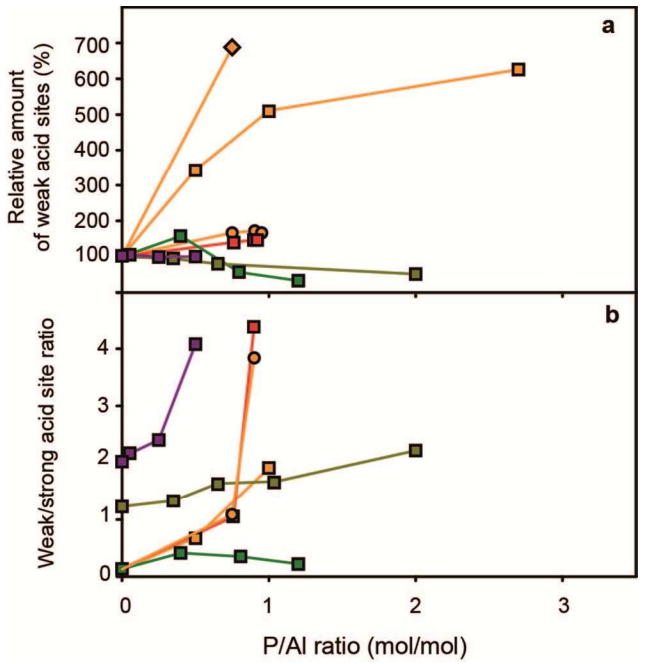

Fig. 7 a) Relative concentration of weak acid sites (%) vs. P/Al ratio b) Strong/weak acid site ratio vs. P/Al ratio. Concentrations are relative to the respective parent H-ZSM-5 material. ■ = Rumplmayr et al. [91] precursor: TMP, probe: pyridine, ■ = Vinek et al. [90] precursor: □ = H_3PO_4, ○ = TMP ◊ = TMPT, probe: pyridine ■ = Jiang et al. [76] precursor: $(NH_4)H_2PO_4$, probe: NH_3 ■ = Lee et al. [78] precursor: H_3PO_4, probe: NH_3, ■ = Caeiro et al. [33], precursor: H_3PO_4, probe: *n*-propylamine

3.2.4 Acid Site Strength Decrease. Phosphorus modification of zeolites does not only decrease the acid site number, but also to a decreases the average acid site strength. [29, 31, 33-36, 50, 53, 54, 57, 60, 63, 64, 66, 68, 69, 74, 76-78, 81-86, 94, 102, 103, 111, 117, 129, 130, 133, 134

Generally, it is reported that the average acid site strength decreases with increasing amounts of phosphorus as can be seen in Figure 7 a and b. The observations originate from three effects.

First of all, the maximum temperature where probe molecules are desorbed from the bridging hydroxyl groups shifts to lower temperatures with increasing phosphorus content, which indicates that these sites decrease in acid site strength. [29, 31, 34, 35, 50, 53, 54, 57, 63-65, 74-77, 85-87, 90, 91, 94, 102, 111] Theoretical calculations have indicated that intramolecular bonds between phosphoric acid and the zeolitic framework lead to a decrease in acid site strength. [104] Conversely, rates of H/D exchange for propene and adsorption of acetonitrile indicated that remaining acid sites in phosphorus modified H-ZSM-5 were not altered in acid site strength. [59, 89]

Second, relative more strong acid sites are affected by phosphatation than weak acid sites. The corresponding increase in weak/strong acid site ratio leads to an overall decrease in average acid site strength. [31, 50, 53, 63, 64, 68, 69, 75-78, 82, 83, 85, 91, 94, 117, 129, 130, 134]

Third, there have been reports where the amount of weak acid sites actually increases. [35, 50, 54, 57, 81, 84, 90] The formation of these new weak acid sites has been attributed to the formation of P-OH groups, hydrogen bonded Si-OH groups in silanol nests and framework incorporated phosphate species. [35, 50, 54, 57, 94] With phosphorus weight loadings above 2 wt.%, P-OH groups and internal Si-OH groups have been observed. [34, 53, 54, 56, 64, 82, 86, 89, 92, 94, 96, 108, 135] It has been reported that these P-OH groups are able to protonate pyridine. [34, 54] In contrast, Rahman et al. reported that P-OH groups have no acidic character and attributed the species to excess phosphates. [96, 97] Other attributions have been P-OH groups in framework incorporated phosphate species and orthophosphoric acid. [56, 58, 87, 92, 94] Nevertheless, at this moment the nature of the weak acid sites that form in phosphated zeolites remains elusive. Systematic studies on these new acid types should be performed in order to attribute them to specific acid sites.

4. Hydrothermal Stability

As was mentioned in the introduction, hydrothermal stabilisation of zeolites is a topic of paramount importance for their use in future clean/green chemical processes. Therefore, we dedicate a separate section of this Review Paper to the promotional role that phosphorus plays on zeolite hydrothermal stabilisation.

4.1 Hydrothermal Stability of Zeolites

Zeolites are metastable as they form under hydrothermal conditions as a transitory phase of quartz. [136] Therefore, continued application of hydrothermal conditions eventually leads to the collapse of their framework structure. In the presence of steam and at temperatures above 400 °C framework Si-O-Al bonds will be gradually hydrolysed and aluminium will be expelled from the framework, forming extra-framework aluminium (EFAl) species (Scheme 3). [105, 106, 137-139] During this process silicon can also be extracted from the framework, leading to the formation of extra-framework silica-alumina.[140] Since Si and Al atoms are extracted from the zeolite lattice, mesopores form and amorphisation the crystal lattice can take place. [5, 138] Due to the removal of negatively charged $[AlO_4]^-$ units from the zeolite lattice, this so-called dealumination will reduce the amount of counter-cations that the zeolitic framework can retain. In the case of H-zeolites, this means that the active sites for catalysis are lost. [141]

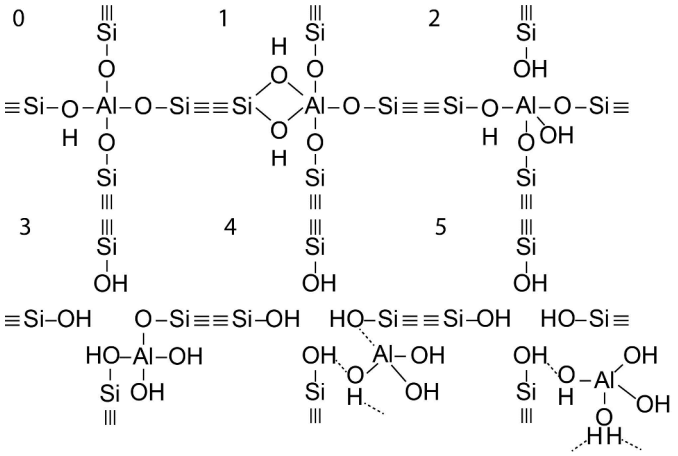

Scheme 3. Reaction steps with intermediate configurations found for dealumination. Solid line is covalent bond. Dashed line is hydrogen bond. Based on Malola et al. [106]

The exact nature of extra-framework aluminium is not clear, but it has been shown to consist of four-, five-, and six-coordinated aluminium species. [138, 142] Furthermore, it has been suggested that extra-framework aluminium can be cationic, which can replace protons in bridging hydroxyl groups. [143, 144] The hydrothermal stability of a zeolite indicates how prone the framework is to dealumination under hydrothermal conditions. Therefore, a zeolite that does not dealuminate and retains acid sites during steam treatment has a high hydrothermal stability. The hydrothermal stability of a zeolite depends on the number of aluminium atoms in the lattice, the framework type, and the type of counter-cations. [138, 145] Increase of temperature, steam volume, or duration of hydrothermal treatment all lead to more severe dealumination. [146, 147]

As was briefly mentioned in the introduction, dealumination poses a challenge in the industrial application of zeolites as acid catalysts. For example, in the FCC process, a regeneration step of the zeolites is performed at high temperatures and in the presence of steam. [25] While this step is effective in the removal of coke deposits, the dealumination induced by steam leads to gradual permanent deactivation of the catalyst. [25, 141] This catalytic deactivation of zeolites will also take place in high temperature reactions where H_2O will form as a reaction by-

product, examples being the methanol-to-hydrocarbons (MTH) process and the dehydration of alcohols. [61, 62] Therefore, hydrothermal stabilization is paramount for the industrial application of zeolites.

For zeolite Y, the most important cracking catalyst, rare earth cations and ultra-stabilization by hydrothermal treatment are used to stabilize the material. [148, 149] In MCM-41, hydrothermal stabilization can be achieved by the addition of salts during synthesis [150 151] In the case of zeolite H-ZSM-5, hydrothermal stabilization can be achieved by the addition of phosphorus. [27, 33, 34, 50, 58] Therefore, most of the studies on phosphorus induced stabilization is performed on H-ZSM-5, although it has been found that zeolite IM-5 can be stabilized by phosphorus as well. [128]

4.2 Hydrothermal Stability Promotion by Phosphorus

4.2.1. Acid Sites. The removal of aluminium from the framework during steaming conditions leads to a loss in active sites. Hydrothermal treatment with temperatures above 750 °C and longer than 5 h, leads to an almost complete disappearance of the bridging hydroxyl groups in zeolites. [34, 58, 108] After hydrothermal treatment of phosphated zeolites it is generally found that Brønsted acid sites are (relatively) better retained in phosphorus modified samples than in their non-phosphated counterparts. [33, 34, 50, 51, 57, 58, 78, 85, 108, 128] If the steam treatment is mild in temperature or time, the total loss of acid site number is only relatively lower in comparison with the non-phosphated samples. However, the absolute number of acid sites is still lower for the phosphated and then steamed samples, than for the parent and steamed samples. [33, 50] This effect was also observed at high phosphorus weight loadings above 3.5 wt.% [85] and is because the phosphatation step already leads to an initial decrease in acid sites as described in section.

If the steam treatment is more severe an absolute higher number of acid sites is remaining for phosphated H-ZSM-5. [33, 34, 50, 51, 57, 58, 78] The phosphorus content plays a role as increasingly higher loadings lead to an increasingly higher number of acid sites being retained after steaming. [34, 51] However, optimal phosphorus loadings have been reported, which lead to a maximum number of strong acid sites being retained as can be seen in Figure 8. [33, 34, 78] The reported corresponding P/Al ratios are different, i.e. 0.5, 0.65 and 1. However, the weight loadings are somewhat more similar, i.e. 1.3 wt.%, [78] 1.4 wt.%, [33] and 2 wt.%. [34] The reason for an optimum in retained strong acid site number most likely stems from the two effects of phosphorus on zeolite H-ZSM-5, i.e. the progressed decrease in acid sites with increasing phosphorus loading on the one hand and the increase of hydrothermal stability on the other. [33] This effect is schematically drawn in Figure 8

Generally, the weak acid site number is not as much affected by steam treatment as the strong acid site number. [33, 50, 51, 57, 64, 75, 78, 108] This phenomenon leads to an even stronger shift towards weaker average acid site strength after steam treatment. Furthermore, Lischke and co-workers showed the formation of a new weak acid site type by following the decomposition of ammonium for steamed NH_4^+ exchanged P/NH_4-ZSM-5 samples. Washing with hot water did not remove this new weak type of Brønsted acid site, but washing with HNO_3 could. The authors attributed the newly formed weak acid type to surface bonded phosphoric acid species, which cannot be removed by hot water washing. [50] This type of weak acid sites were confirmed in another work and also attributed to (pyro) phosphoric acid. [33]

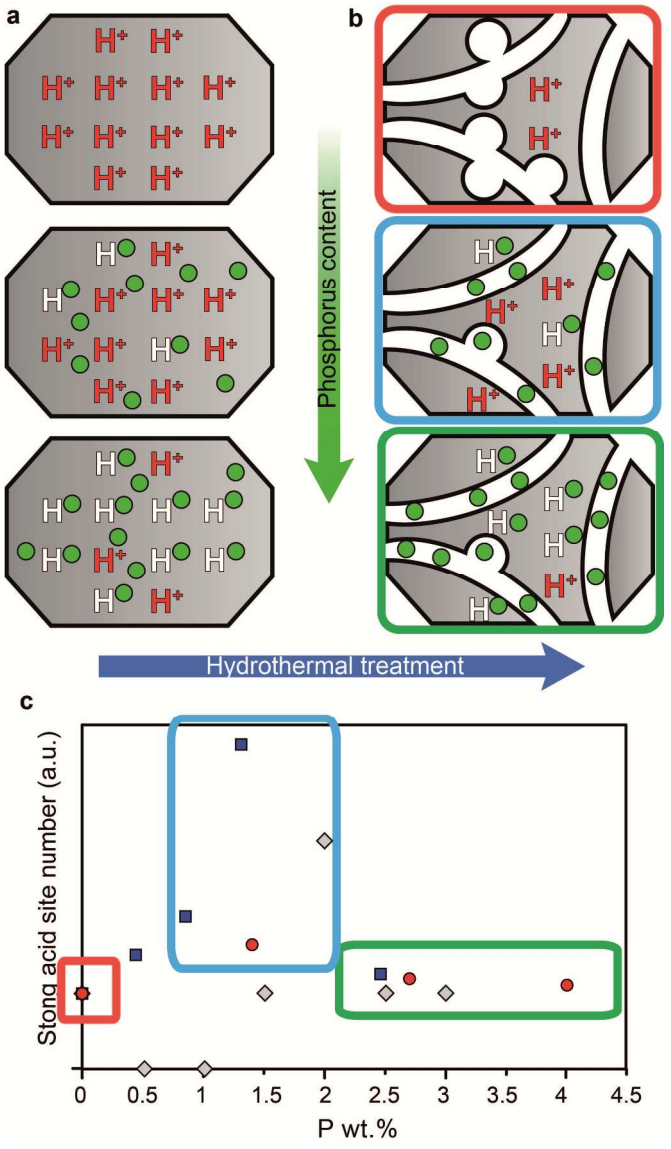

Fig. 8 Schematic representation of the promoting effect on acid site number during hydrothermal treatment with increasing phosphorus weight loading. The number of strong acid site is normalized to the amount of acid sites for the parent material after hydrothermal treatment. ■ = Caeiro et al. [33] ■ = Lee et al. [78] ■ = Blasco et al. [34]

4.2.2. Porosity. The (relative) change in micropore volume and surface area after steaming is less for phosphorus-modified

samples when compared to their non-phosphated counterpart. [33, 34, 78, 102, 108] This is in line with the retarding effect that phosphorus has on dealumination. There are reports for phosphated zeolites with phosphorus content above 1 wt.% where the micropore volume and area increase after post-steam treatment. [34, 57, 75, 78, 87, 108] After hydrothermal treatment of phosphated H-ZSM-5, 94% of phosphorus could be eluted by washing in NH_4F. However, the amount of surface area and micropore volume only increased with less than 6% [19] and no increase in surface area and micropore volume was retrieved after washing with hot water. [85, 108] These results indicate that phosphorus actually prevents the destruction of micropores, instead of filling newly formed mesopores.

4.2.3. Effect of hydrothermal treatment on phosphorus species. X-ray photoelectron spectroscopy (XPS) measurements showed a 55% increase of phosphorus species on the surface of 2 wt.% phosphated H-ZSM-5 after steam-treatment. [51] This would indicate that phosphorus migrates to the surface during steaming. Chemical analysis has shown that 5-10% of phosphorus species disappear after hydrothermal treatment. [57] With increasing phosphorus content, the $P_{Surface}/P_{Bulk}$ ratio decreased for hydrothermally treated samples, i.e. with increasing phosphorus weight loadings more phosphorus was found in the bulk. [51] Unfortunately the $P_{Surface}/P_{Bulk}$ ratios before steaming were not given in the work. However, if we keep the model of from Figure 2 in mind, the latter finding would indicate that phosphorus migrates outward, but also inwards the zeolite depending on the weight loading. Furthermore, X-ray absorption microscopy results showed that phosphorus species are more homogenously distributed after steam-treatment, indicating that phosphorus species move into the zeolite. [87] This contradiction deserves more careful study.

After post-steam treatment the amount of smaller phosphate species decreases and the amount of more condensed polyphosphate species increases. [33, 34, 50, 55, 57, 58, 64, 78, 85] The condensed species can be reduced after a washing step, which would indicate either that the condensed species are washed out, or hydrolysed into smaller species. [50, 59, 85] Furthermore, spectroscopic results indicate that most phosphorus appears to be present in local SAPO interfaces. [33, 34, 50, 55, 57, 58, 64, 78, 85] Especially for samples with P/Al ratios above 0.6. [33, 34, 50, 55, 57, 58, 64, 78, 85]

4.2.4. Framework aluminium stabilisation. For phosphated zeolites the decrease in the number of Si-O-Al bonds, i.e. the decrease in TFAl species and the formation of EFAl species during steaming, is reduced, further confirming that phosphorus stabilizes TFAl species. [34, 50, 58, 75, 78] In two reports, the reduced decrease in the number of TFAl species during steam treatment for phosphated H-ZSM-5 was only relative when compared to non-phosphated H-ZSM-5 and the absolute number of TFAl species after steam treatment remained higher for the non-phosphated samples. This holds even for samples that were steamed under severe conditions. [33, 71] It was found that the migration of aluminium to external surface decreases during steaming with increasing amounts of phosphorus loading. [51] This indicates that phosphorus either prohibits the migration of aluminium species, or prevents dealumination altogether. Several studies have shown that local SAPO interfaces are not affected by steam treatment.[33, 34, 55, 58, 71, 78, 85, 87, 108]

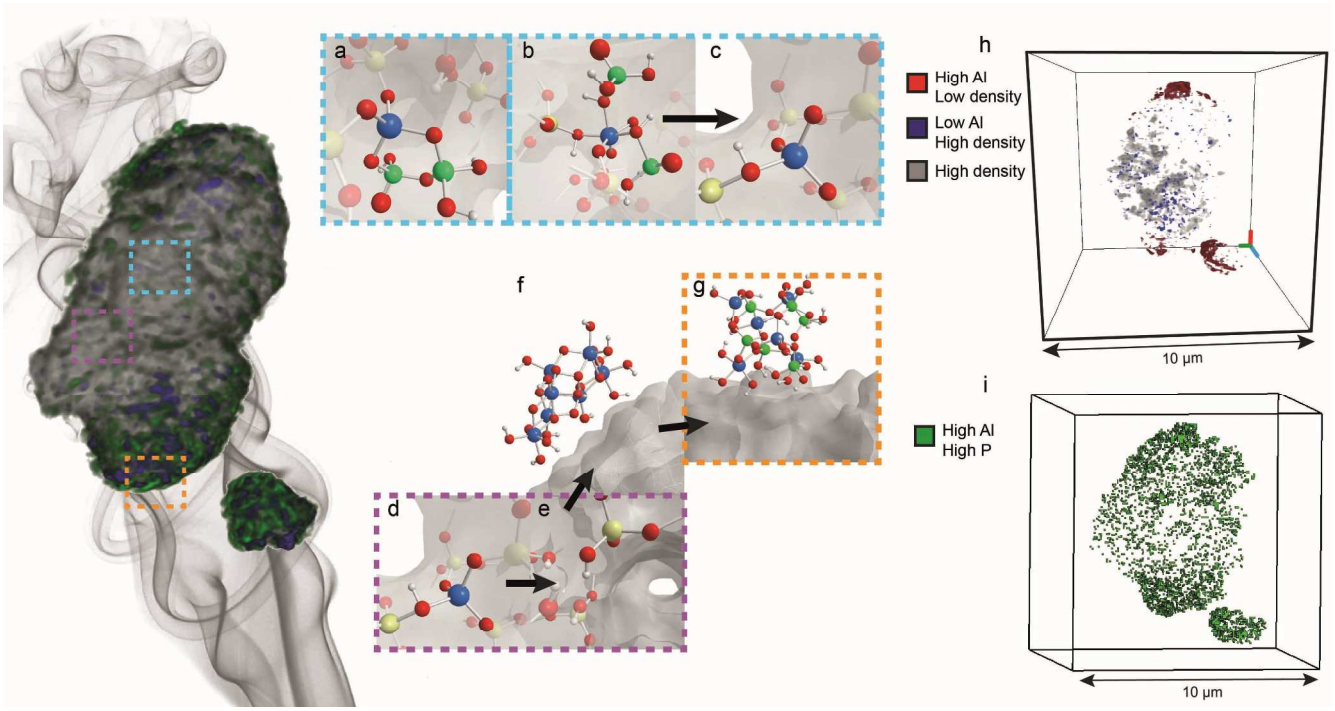

Fig. 9 Phosphated and steamed H-ZSM-5 sample from reference [108] and the main effects that take place during steam treatment. (a) Local framework SAPO interfaces are not affected by steam treatment and remain in the framework. (b) Physically coordinated TFAl species are also resistant to steam, while (c) removal of the physically coordinated phosphates by hot water washing leads to acid site retrieval. (d) TFAl atoms that are not interacting with phosphorus are (e) expelled from the framework and (f) migrate as AlO(OH) species to the surface, where they (g) react with phosphates to form aluminium phosphates. (h) Statistical analysis on the particle showing the presence of enriched Al zones on the external surface and Al depleted regions in the crystal interior. (i) Statistical analysis on the particle showing high concentrations of phosphorus and aluminium on the external surface, indicating the presence of extra-framework $AlPO_4$ islands that form on the surface.

A recent 3-D X-ray tomography study shown in Figure 9 indicated that local SAPO interfaces are located throughout zeolite H-ZSM-5 and hold aluminium atoms fixed in the framework, which was previously suggested by Zhuang et al. and Damodaran and co-workers. [55, 58, 71] This explains why the pore-structure of the zeolite remains intact during steam treatment. The study further showed that the location of phosphorus plays an important role in the hydrothermal stabilization phenomenon. As was previously discussed, phosphorus forms a gradient and does not penetrate completely into the zeolite interior. Therefore, aluminium atoms that are located far from the external surface will not be in the presence of phosphorus. [55, 71, 86, 87] Consequently, these classic TFAl atoms are expelled from the framework during hydrothermal treatment. [33, 34, 55, 71, 85-87, 108] High steaming temperatures and H_2O lead to the migration of this extra-framework aluminium to the external surface of the zeolite, where these species react with excess phosphorus to form $AlPO_4$.[33, 34, 51, 55, 71, 108, 152, 153] This means that phosphate species also effectively act as a sink for EFAl species, which is another possible promotional effect of phosphorus. [92] As EFAl species have been suggested be present as debris in the pores and form cationic Al species that replace protons on bridging oxygen groups, removal of these species could explain the higher retained strong acid number. [137, 154]

The improved hydrothermal stability of H-ZSM-5 after phosphatation (or SAPO-fication) can be rationalized by the presence of the local SAPO interfaces. It is well known that SAPO materials are extremely hydrothermally stable and have been reported to withstand temperatures up to 1000 °C in steam, without significant loss of crystal structure. [155-157] Therefore, the formation of SAPO patches throughout the zeolite framework reinforces its structure, keeping the framework intact for prolonged exposure to hydrothermal conditions.

Nevertheless, although phosphorus has a promoting effect on the hydrothermal stability of TFAl species, increasing times and temperatures of the hydrothermal treatment eventually leads to the complete removal of aluminium species from the framework. As hydrothermal treatment gradually breaks all Si-O-Al bonds of one aluminium site, more Al-O-P bonds are being formed in the presence of phosphorus. [58, 71, 105] For steam treatments at elevated temperatures and prolonged times the formation of an extra-framework crystalline $AlPO_4$ phase has been observed. [58, 85] Crystalline $AlPO_4$ is only formed during severe steaming conditions, as $AlPO_4$ is not observed after steaming P/H-ZSM-5 at temperatures lower than 760 °C for less than 2 h. [55, 58, 71, 87, 108] However, in the case of Caeiro and co-workers, an $AlPO_4$ phase was not observed even after 20 h of steaming phosphated H-ZSM-5 at 800 °C. [33]

It is important to realise that local SAPO interfaces do not prevent dealumination during hydrothermal treatment altogether, but most likely retards the process shown in Scheme 3. The formation of $AlPO_4$ is gradual as presented in Figure 10.

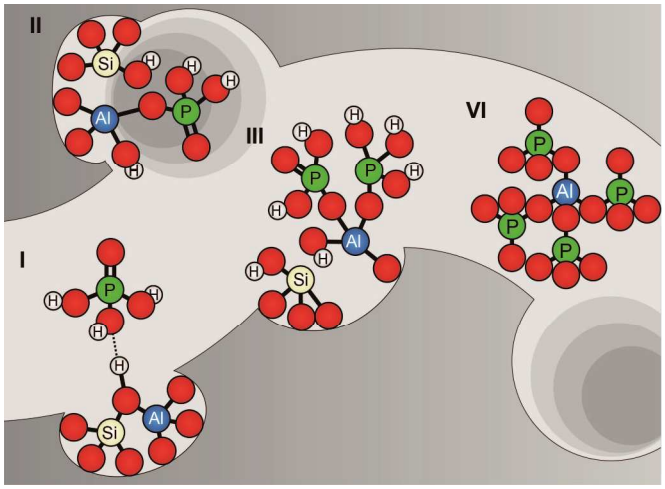

Fig. 10 Proposed model of different stages of dealumination in the presence of phosphorus. Model has been based on suggestions by Abubakar et al., Zhuang et al., and Cabral de Menezes et al. [58, 59, 71]

4.2.5. Reversible decrease in acid sites after steaming. Hydrothermal treatment of H-ZSM-5 and P/H-ZSM-5 reduced strong acid sites for both samples. However, it has been found that elution of phosphorus after hydrothermal treatment leads to a recovery of strong acid sites. When a sample was phosphated and then post-steam treated at 700 °C for 0.5 h, the amount of phosphorus that could be removed from the sample by washing was 60%. [50] Before elution of P/H-ZSM-5 the number of acid sites that remained was only 13% of the parent material. After elution the concentration of acid sites increased to 42% of the parent material. Steamed and washed P/H-ZSM-5 had 114% more strong acid sites than steamed H-ZSM-5. Other experiments on the elution of phosphorus from hydrothermally treated P/H-ZSM-5 confirmed these results. [34, 85, 108] Acid sites of steamed non-phosphated materials could not be retrieved after washing with NH_4F. [34] The retrieval of acid site number by washing is shown in Figure 11.

In addition, Liu and co-workers found a small quantity of a new type of strong Brønsted acid site to be formed after a steam and washing step. [85] They reported that a consecutive steam treatment removed the acid site, while a following washing step caused it to reappear again. Similar to the retrieval of acid sites, after hydrothermal treatment, the amount of TFAl species that can be recovered by elution of phosphorus is much lower than before steaming. [50] Still, a considerable amount of aluminium species can be retrieved as TFAl species. That is, of the 30% of the original amount of TFAl species that remained after steaming P/H-ZSM-5 at mild conditions, 70% of the original amount of TFAl species could be obtained after washing. With increasing severity of the hydrothermal treatment conditions, this amount decreased, i.e. from 15% of the original amount of TFAl species after steaming to 30% of the original amount of TFAl species after washing, as is shown in Figure 11. [50] Similar results have been reported in other works. [85, 108]

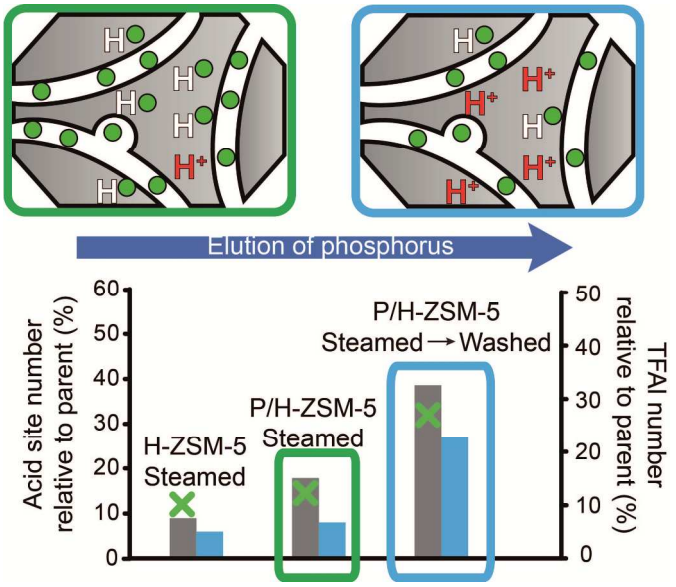

Fig. 11 Schematic representation of the retrieval of acid site number and TFAl species by washing after hydrothermal treatment. The acid site number is a relative to the respective parent materials. Left axis: Acid site number was determined using pyridine adsorption. ■ = Lischke et al. [50] (Steamed at 700 °C for 30 min. Washed using hot water) ■ = Blasco et al. [34] (Steamed at 750 °C for 5 h. Washed using NH_4F) Right axis: TFAl number was determined using ^{27}Al MAS NMR. ■ = Lischke et al. (Steamed at 700 °C for 30 min. Washed using hot water) [50]

Although these findings are not quite understood at the moment, an important consequence of the recovery of strong acid site number after washing is that the hydrothermal stabilization effect of phosphorus does not seem to require irreversible phosphorus aluminium interactions. Recently, a study performed by our group has shown that the retrieval of strong acid sites and TFAl species is concomitant with the decrease in lattice aluminium that was induced to six-coordination by phosphates. [85, 108] These findings indicate that TFAl atoms, which adopt a six-fold coordination in the presence of phosphates species are hydrothermally stabilized as well.

4.2.6. Only for zeolite H-ZSM-5? As was mentioned the local SAPO interfaces have been found to remain unaffected during steam treatment and as aluminium remained fixed in the framework, the pore structure was better retained. However eventually, with prolonged steam treatments all Si-O-Al bonds of the SAPO interfaces are hydrolysed, leading to the formation of extra-framework $AlPO_4$. [58] Therefore, it would seem that SAPO interfaces form metastable intermediates during dealumination in the zeolite H-ZSM-5 channel system. We explicitly mention the zeolite ZSM-5 channel system, as it is

not certain if phosphorus has a similar promoting effect on very different framework topologies. In a contribution from Costa and co-workers it can be seen that for zeolite H-beta and H-mordenite phosphatation followed by hydrothermal treatment only leads to extra-framework crystalline $AlPO_4$ formation. [30] Authors from the same group applied a similar steam treatment on phosphated H-ZSM-5 and the spectroscopic signatures of SAPO interfaces could be seen. [33] This begs the question if the local SAPO interfaces in H-ZSM-5 are inherently stabilized by the MFI channel system, while not in other topologies, where only extra-framework $AlPO_4$ would form. It could explain why reports in the academic and patent literature on phosphorus modification are almost exclusively based on zeolite H-ZSM-5 or similar multidimensional 10-MR structures, such as ZSM-11, MCM-22, ITQ-13 and IM-5.[82, 111, 113, 128] Already, the phosphatation of ZSM-5/ZSM-11 intergrowth structures lead to higher dealumination rates after phosphatation than H-ZSM-5. [82] On the other hand, it has been reported that phosphorus modification of the mesoporous material MCM-41 led to significant hydrothermal stabilization. [158] We hope to see future systematic studies that will shed new light on these scientifically pertinent questions. Computational studies such as performed by Svelle et al. and Lisboa and co-workers could shed new light on the actual stabilizing effect that the proposed phosphorus-aluminum interactions induce on the framework.[105, 139, 159]

5. Phosphorus and Zeolite-based Catalysis

In the previous sections we have shown that phosphorus affects the acidity, porosity and hydrothermal stability of zeolites. As expected this has a profound effect on the catalytic properties of zeolites in a variety of catalytic processes, as can be read in the following sections. However, since catalytic conditions and materials differ in most of the literature, direct comparisons concerning performance are almost impossible to make. Therefore, all comparisons and figures in the following section are only meant to show rough trends and the reader should keep in mind that differences between e.g. reaction temperature, conversion, Si/Al ratio, crystal size and space velocity have not been taken into account.

5.1 Automotive Catalysis

Transition metal exchanged zeolites are used in automotive catalysis to remove NO_x formed during the combustion of transportation fuels, and are especially suited for diesel engines. [4, 37, 160] The process is known as Ammonia Selective Catalytic Reduction (NH_3-SCR), and examples of catalysts are Fe-ZSM-5, Fe-Beta and Cu-SSZ-13, although small-pore zeolites such as SSZ-13 were found to be most active. [4, 37, 65] In short, NO is oxidised into NO_2 by transition metal ions (TMI), e.g. Fe^{3+} and Cu^{2+}, which act as redox centres. [160, 161] When NO or NO_2 reacts with NH_3 chemisorbed on Brønsted acid sites, N_2 and H_2O are formed. [160, 161]

Deactivation of NH_3-SCR zeolite catalysts during operation occurs mainly by thermal conditions and chemical poisoning. [4] Although many chemicals present in the feed, e.g. Pt, Zn, and Ca, poison the catalyst, poisoning by phosphorus is especially deleterious. [37, 162] Phosphorus compounds are present in lubricant oils and biofuels and come into contact with the zeolite catalyst during operation. [65] NH_3-SCR zeolites that are treated with phosphorus show a strong decrease in $DeNO_x$ activity. [32, 37, 65, 162] It was found that there is a linear relationship between phosphorus content and decrease in activity. [32]

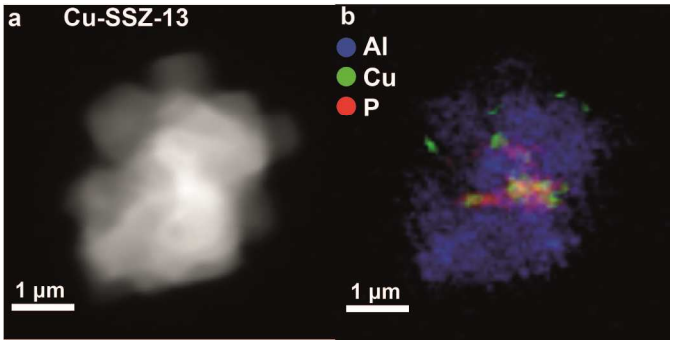

Fig. 12 X-ray absorption microscopy results of a phosphorus poisoned Cu-SSZ-13 crystal agglomerate (0.34 mmol/g zeolite). It can be seen that phosphorus and copper are located on the external surface of the agglomerated squares. Adapted from reference [37]

The effective poisoning with phosphorus is caused by several deactivation mechanisms, which are related to the previously discussed physicochemical changes induced by phosphorus. [37] First of all, there is a decreased amount of NH_3 that can be chemisorbed. [32, 37, 65, 162] This can be attributed to a loss in acid sites and to blocking of active sites by phosphate species. However, it was found that the decrease in NH_3 uptake was only minor to the decrease in chemisorbed NO and NO_2 species and is therefore only a partial contributor to the catalyst deactivation. [65, 162]

The decrease in chemisorbed NO_x species indicates that there is a decrease in TMI centres, which was confirmed by an increase in Fe^{2+} and CuO species after phosphorus introduction. [37, 65] Furthermore, it was found that after phosphorus modification Fe^{2+} could not be reduced to Fe^0 at low temperatures. [162] In the case of Fe, it was suggested that Fe^{3+} reacts with phosphorus. [65, 162] However, another explanation for the observed effects was suggested to arise by partial dealumination caused by phosphorus. [37] In this manner the framework negativity decreases and Cu^{2+} counter cations are forced into CuO agglomerates. It was further observed that these CuO agglomerates moved out of the zeolite and were deposited on the external surface as can be seen in Figure 12. [37] Their presence was suggested to decrease the accessibility of the material even more. While further studies should be performed to distinguish the exact effect of phosphorus-TMI interactions, the decrease in acid sites, dealumination and pore

blocking all follow from previously discussed phosphorus-zeolite interactions. The attraction between phosphorus and framework aluminium and the formation of neutral SAPO interfaces is a good explanation why phosphorus is a much more effective poison than Zn, Pt, and Ca.

5.2 Hydrocarbon Catalysis

Protonation by Brønsted acid sites of C-C bonds, C-H bonds, or –OH groups in hydrocarbons and alcohols leads to the formation of carbonium, carbenium, or oxonium groups. [163-165] Subsequently, these groups can be cracked, dehydrogenated, dehydrated, isomerised, or oligomerised. As H-zeolites have Brønsted acid sites and shape-selective properties, they are widely used in industry in these types of reactions to produce hydrocarbons. Changes induced by phosphorus on the number and strength of acid sites and the shape selectivity leads to different catalytic properties. Furthermore, catalytic lifetime is improved as the hydrothermal stability increases for phosphated materials.

5.2.1 Effect of Acid Site Loss. The decrease in acid site number and strength caused by phosphatation has obvious effects on hydrocarbon catalysis performed by zeolites. It can be expected that a reduction in Brønsted acid sites, i.e. the active sites in acid-catalysed reactions, leads to a decrease in catalytic activity. Certainly, this effect can be observed for several hydrocarbon catalysis processes as shown in Figure 13 a-b, as the progressed reduction in the number of Brønsted acid sites with increasing phosphorus content, leads to a decrease in activity in the catalytic cracking of hydrocarbons, [33, 34, 57, 64, 76, 79, 85, 90, 97, 99, 111, 128] alcohol dehydration [20, 21, 24, 38] and methanol-to-hydrocarbon reaction. [29, 31, 59, 82, 96, 97, 103, 113]

For the cracking of alkanes, it was established that there is indeed a linear correlation between strong Brønsted acid site number and cracking activity in phosphated zeolites. [33, 90] In the case of methanol-to-hydrocarbons and alcohol dehydration, 100% conversion can be obtained with increasing temperatures. [29, 31, 59, 77, 81-84, 96, 97, 103, 113] For the MTH reaction these results are not surprising as Hunger and co-workers showed that zeolite materials with very low Brønsted acid site number could reach 100% methanol conversion at 400 °C. [166]

Besides activity, a decrease in acid site number can change the selectivity in hydrocarbon catalysis reactions as well, provided that it reduces the chance of secondary reactions. This is shown in Figure 13 c-d For the MTH reaction, selectivity towards light olefins and especially propylene increases for unmodified zeolite materials with low acid site number. [31, 59, 113, 166-168] It has been suggested that low acid site density reduces the chance that the primary MTH products (light olefins) undergo hydride transfer and cyclisation reactions during diffusion, thus decreasing the formation of larger products. [31, 168, 169] In agreement to this, the observed decrease of strong acid sites in phosphated zeolites leads to an improved selectivity toward light olefins in the MTH reaction. [29, 31, 59, 82, 96, 97, 103, 113] In Figure 13 d it can be observed that the selectivity towards light olefins increases with increasing phosphorus loadings, i.e. decreasing acid site number.

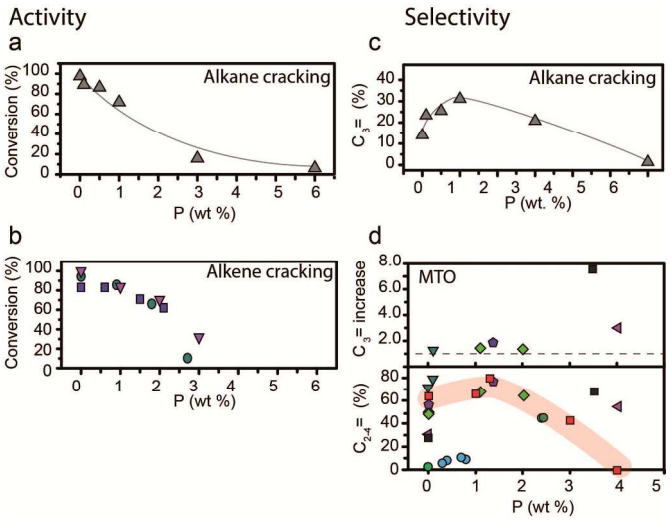

Fig. 13 Effect of phosphorus weight loading on (a) Alkane cracking activity, conversion of reactant. [76] (b) Alkene cracking, conversion of reactant. ■ = Zhao et al. [64] ■ = Xue et al. [57] ■ = Xue et al. [79] Differences between reaction temperature, Si/Al ratio, crystal size and space velocity have not been taken into account. (c) Alkane cracking selectivity, propylene selectivity (%) [76] (c) Methanol-to-olefins (MTO) selectvitiy, propylene selectivity increase. The increase in propylene selectivity is relative to that of the respective parent material. (d) Actual C_2-C_4 selectivity vs. phosphorus weight loading in MTO. ■ = Kaeding et al. [52] ■ = Rahman et al. [68] ■ = Rahman et al. [69] ■ = Vedrine et al. [29] ■ = Abubakar et al. [59] ■ = Liu et al. [31] ■ = Li et al. [82] ■ = Dyballa et al. [89] The red highlight focusses on a trend on an optimum phosphorus loading reported in reference 61. Reaction temperatures are between 400 °C and 460 °C. Differences between Si/Al ratio, crystal size and space velocity have not been taken into account.

It is expected that the decrease in acid site number also influences the product selectivity in catalytic cracking of alkanes. Catalytic cracking over zeolites with a low acid site number is generally follows the protolytic cracking route (monomolecular mechanism).[170] This is because low acid site density reduces the chance that alkanes react with carbenium ions (bimolecular mechanism).[171] The bimolecular mechanism is in essence a secondary reaction of the monomolecular pathway since carbenium ions are formed in the latter. [163, 164, 172, 173] For more information on monomolecular and bimolecular cracking mechanisms we refer the reader to some of the excellent reviews that have been written on the subject. [163, 164, 172, 173]

Nevertheless, typical products that are formed by the monomolecular cracking mechanism are methane, ethane, propylene, hydrogen and high olefin/paraffin ($C^=$/C) product ratios.[164, 170] Whereas the bimolecular cracking mechanism produces more paraffins, less olefins and more branched C_{4+} products. Therefore, phosphated materials are expected to show a product distribution that corresponds to the monomolecular cracking mechanism. Indeed, as can be seen in Figure 13 c, phosphated zeolites applied in alkane cracking show an increased selectivity towards light olefins. [33, 76, 85, 97, 101, 108] However, when high alkane cracking temperatures are applied,

i.e. more than 650 °C, product distributions are very similar for phosphated and unmodified H-ZSM-5, as at these high temperatures carbenium ions become unstable and the monomolecular mechanism is dominant. [172, 174]

5.2.1 Effect of Weak Acid Sites. A decrease in average acid site strength is not expected to have a strong influence on the product distribution in the methanol-to-hydrocarbon reaction and catalytic cracking of alkanes. [1, 172] Although weak Brønsted acid sites are able to crack alkanes, they were found to have turn-over frequencies that were three orders of magnitude smaller than those found for strong Brønsted acid sites. [90] In a study by Bleken and co-workers, no significant effect of acid site strength was found for the product distribution in the MTH reaction. [175]

However, the formation of weak acid sites does have a pronounced effect on the catalytic performance in the cracking of alkenes and the dehydration of alcohols. For the cracking of alkenes, the modification of zeolites with phosphorus leads to an increase in propylene product yield. [57, 64, 66, 79, 102, 111] Lin and co-workers showed in their study that the weak acid sites that form during phosphatation prefer a different reaction pathway than strong acid sites, leading to higher propylene yields. [66] Higher phosphorus loadings, i.e. lower average acid site strength, lead to a higher selectivity toward propylene. [66] However, as can be seen in Figure 14 b, the selectivity towards propylene decrease after phosphorus weight loadings reach above 2 wt.%. [57, 64, 79, 102]

For the dehydration of alcohols, the selectivity towards ethylene increases with increasing phosphorus content and reaction temperature, as shown in Figure 14 a. [63, 77, 81, 83, 84, 176] If all strong acid sites are removed, at weight loadings above 3 wt.% the selectivity towards ethylene reaches 99.4% as only dehydration takes place. [63, 77, 81, 83, 84] If the catalyst still contains a small amount of strong Brønsted acid sites, higher hydrocarbons are also detected. At weight loadings of 1.3-1.9 wt.% P the selectivity towards propylene has been reported to obtain a maximum and can reach up to 33% at temperatures between 400 °C and 500 °C. [63, 81, 84, 176] Propylene selectivity is maintained with time-on-stream, while the unmodified material gradually loses selectivity.[63]

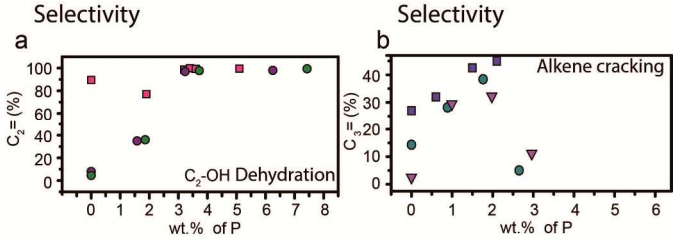

Fig. 14 Effect of phosphorus weight loading on (a) ethanol dehydration, ethylene selectivity at temperatures > 400 °C ■ = Zhang et al.[77] ■ = Ramesh et al.[81] ■ = Ramesh et al.[84] Differences between reaction temperature, Si/Al ratio, crystal size and space velocity have not been taken into account. (b) Alkene cracking, propylene selectivity (%). ■ = Zhao et al. [64] ■ = Xue et al. [57] ■ = Xue et al. [79] Differences between reaction temperature, Si/Al ratio, crystal size and space velocity have not been taken into account.

Summarising the effect of changes in acidity on catalysis; the decrease in acid site number has a promotional effect on the methanol-to-hydrocarbons reaction selectivity toward light olefins, especially propylene. The decrease in acid site strength improves the pure dehydration of alcohols-to-olefins. For the cracking of hydrocarbons, both the decrease in acid site strength (alkenes) and acid site number (alkanes) leads to an improved selectivity towards light olefins, especially propylene.

5.2.3 Changes in Shape-Selectivity. So far, one can wonder if the addition of phosphorus does nothing more than decrease the acid site number and strength, and if an unmodified zeolite with similar acidic properties is just as effective in altering the catalytic performance. However, phosphorus addition changes zeolites – and specifically H-ZSM-5 - in an even more profound way, i.e. it changes the shape-selectivity. This is because of the presence of phosphates in the micropore channel system, where they form diffusion barriers and inhibit the formation of voluminous (intermediate) species.

This effect is especially obvious in the alkylation and disproportionation of aromatics, as shown in Figure 15 a. The addition of phosphorus to H-ZSM-5 boosts the selectivity towards *p*-xylene to 95%. [10, 17, 36, 70, 90, 93, 95] In general, the increase in selectivity can be attributed to the effective reduction in pore size for channels, channel intersections and in pore openings. [10, 17, 95] The bulkier *o*- and *m*-xylenes will diffuse slower out of the pores and the rapid decrease in concentration of *p*-xylenes will promote the isomerization of the former two isomers into the latter. In a recent work by Janardhan et al. it was found that washing out excess phosphorus from the pores improved the activity in aromatic alkylation and disproportionation, as pore blocking was reduced. However, the selectivity still remained 95% for *p*-isomers. This indicates that phosphates which are irreversibly connected to the framework, are responsible for a decrease in pore volume, restricting the formation and diffusion of the bulkier *ortho* and *meta* isomers.[36]

The presence of phosphates in the zeolite channels also has an effect on the product distribution in alkane cracking and methanol-to-hydrocarbons. If one compares the product distributions of phosphated multi-dimensional 10-MR zeolites in the methanol-to-hydrocarbon reaction at 400 °C it can be observed that there is an increase in alkene selectivity, a decrease in aromatic selectivity and an increase in C_{3+} species.[29, 52, 59, 82, 113] The strong decrease in aromatic species is not observed for zeolites with low acid site number and can therefore be attributed to the presence of phosphorus species.[59] Interestingly, similar product distribution were reported for methanol-to-olefins over zeolite H-ZSM-22, which has a 1-dimensional pore system and no channel intersections.[177] In the latter topology a decrease in ethylene selectivity was also observed, which can also be found in the studies of Kaeding et

al. [52] and Abubakar and co-workers [59], but not for the other works. Nevertheless, an important suggestion to make is that, although phosphorus modification alters the acidity of zeolites, it appears that the change in topology plays a major role in its selective properties as well, especially reducing the presence of aromatics in the product stream.

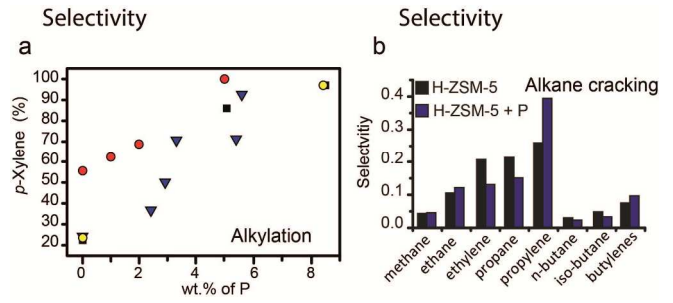

Fig. 15 Effect of phosphorus weight loading on (a) alkylation of toluene, *p*-Xylene selectivity(%). ■ = Chen et al. [7] ■ = Young et al. [11] ■ = Kaeding et al. [17] ■ = Vinek et al. [90] Differences between reaction temperature, Si/Al ratio, crystal size and space velocity have not been taken into account. (b) Alkane cracking, selectivity in moles of the main products formed during the catalytic cracking of n-hexane over a full temperature program ■ = H-ZSM-5 ■ = Phosphated steamed and eluted H-ZSM-5. [108]

In a recent study performed by our group we found the product distributions for n-hexane cracking over phosphated H-ZSM-5 resembles that of zeolites that are 1-dimensional along 10-member ring (MR) channels, such as H-ZSM-22 and H-ferrierite.[108, 178, 179] Similar to these materials an increase in methane, ethane, propylene, butylene and a decrease in ethylene, butane and pentane selectivity was observed, as can be seen in Figure 15 b.

As was mentioned in the previous section, this shift in product distribution for alkane cracking is typical when the monomolecular cracking mechanism becomes more dominant. [164] The change in product distribution in the MTH reaction stems from a larger contribution of the alkene cracking cycle. [1, 177] This change in mechanism in both catalytic processes, stems from the same origin. More specifically, the change in selectivity follows from the ability of a zeolitic framework to stabilize carbenium ions, which are the intermediate species in the bimolecular cracking mechanism and the aromatic-based cycle in MTH. [1, 164, 172, 177] For unmodified multidimensional medium pore zeolites, the channel intersections can more successfully stabilize these voluminous carbenium ions. [170, 172, 180] However, phosphates - presumably connected to local SAPO interfaces - present in the channel intersections will hinder the formation of voluminous carbenium ions. This can be observed in one study on H-MCM-22, where after phosphorus modification a decrease in the formation of enyl carbenium ions is observed during the MTH reaction. [113]

Summarizing, it is plausible that the presence of phosphate species supresses the aromatic-based hydrocarbon pool mechanism during the MTH process, while in the catalytic cracking of alkanes the bimolecular cracking mechanism is inhibited. Whether this is considered a promotional or poisonous effect of phosphorus depends on the desired product distributions.

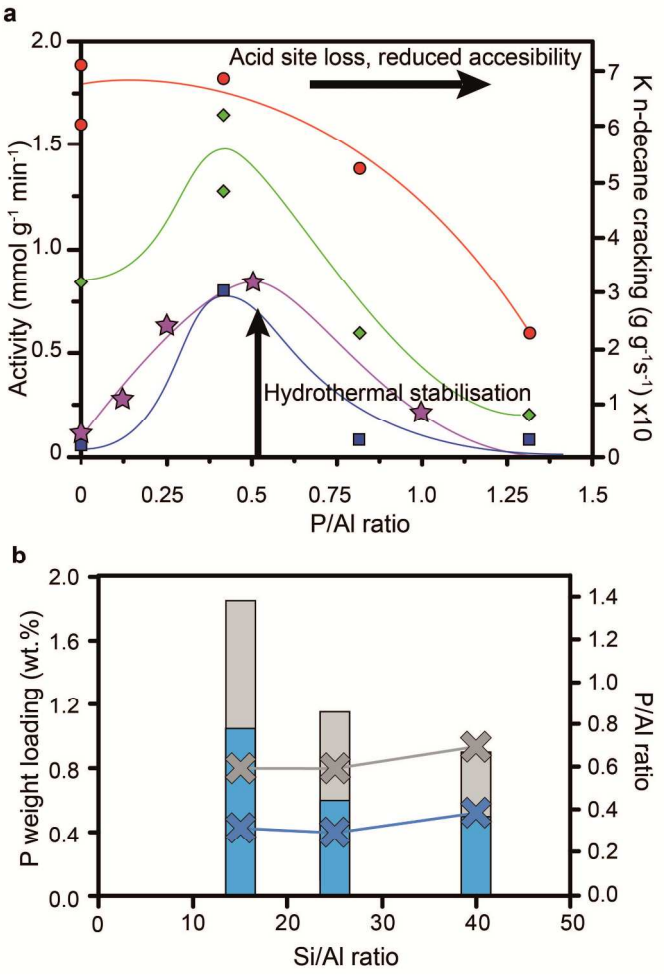

Fig. 16 (a) Effect of phosphorus and post steam treatment on the cracking of n-hexane [33] (left axis) and n-decane [34] (right axis) by H-ZSM-5. Adapted from reference 18. Activity is plotted against phosphorus weight loading (H_3PO_4 precursor). Left axis [33]: ■ = H-ZSM-5 (Si/Al = 13). ■ = H-ZSM-5 steamed at 800 °C for 5 h. ■ = H-ZSM-5 steamed at 800 °C for 20 h. Reaction temperature is 500 °C. Right axis [34]: ■ = H-ZSM-5 (Si/Al = 25) steamed at 750 °C for 5 h. Reaction temperature is 500 °C. Lines are not fits and meant to guide to eye. (b) ■ = Optimal average cumulative catalytic conversion during naphta cracking with additional H_2O in the feed at 650 °C after 1 h for H-ZSM-5 with different Si/Al ratios vs P weight loadings and P/Al ratios ($NH_4H_2PO_4$ precursor) .[88] ■ = Optimal first order kinetic rate constants in n-decane cracking of H-ZSM-5 steamed at 750 °C for 5 h. [34] Left axis in bars: Phosphorus weight loading. Right axis as crosses with lines: P/Al ratio

5.2.3 Improved Catalytic Stability. The addition of phosphorus to zeolites has been reported to lead to a decrease in coke formation in hydrocarbon catalysis. [31, 63, 64, 77, 81, 84, 108] It is expected that the decrease in acid site number and strength reduces the chance that products undergo hydride transfer and cyclisation reactions.[31, 63, 77, 81, 84] Moreover, as the formation of

carbenium ions is inhibited due to low acid site number and steric constraints, coke formation is expected to decrease. [172, 181, 182] Not surprisingly, the decrease in coke formation leads to increased catalytic lifetime. [31, 64, 77]

However, the major reason for improved catalytic lifetime is the improved hydrothermal stability induced by phosphorus. After hydrothermal treatment, phosphorus modified samples have higher catalytic activities than their non-phosphated counterparts. [33, 34, 57, 60, 64, 75, 78, 79, 85, 88, 108, 174] If reactions are performed under hydrothermal conditions, phosphated catalyst maintain activity for longer time-on-stream.[60, 63, 64, 88, 128, 176] Samples that were eluted of phosphorus after steaming regained strong acid sites and consequently the cracking activity increased. [34, 85, 108]

As we have read in section 4.2 phosphated zeolites are expected to perform better in catalysis after steam treatment than their non-phosphated counterparts, because they contain more strong acid sites. However, the direct link between strong acid site number and cracking activity is not as straightforward after hydrothermal treatment. Samples with high phosphorus weight loadings and a higher strong acid site number after hydrothermal treatment, had lower cracking activity than samples with lower phosphorus weight loadings and lower or equal acid site number. [34] Furthermore, it was found that steamed parent H-ZSM-5 had a higher number of Brønsted acid sites, while steamed phosphated H-ZSM-5 had a lower amount. Interestingly, the cracking activity for the latter sample was higher. [33] Therefore, other factors such as acid site distribution, accessibility and limitations in coke formation will probably play a role. [33] In the cracking of alkenes, it was reported that hydrothermal treatment increased the activity for phosphated samples, which would indicate that the accessibility of the phosphated zeolite improves after steam treatment. [57, 79]

As was mentioned in section 4, adding more phosphorus is not the key in retaining more active sites after steaming, as there are several (varying) optimum phosphorus loadings (as is shown in Figure 16 a and b). [33, 34, 57, 60, 75, 78, 79, 88] In line with what was discussed in sections 3-4, phosphatation leads to pore-blockage, reduced accessibility and loss in acid site number, which is amplified with increasing phosphorus loadings. Therefore, a decrease in cracking activity is expected with increasing phosphorus content. However, after steaming the promotion of hydrothermal stability by phosphorus comes into effect. As such, when comparing a steamed phosphated sample with a steamed non-phosphated sample, the former will perform better in cracking, especially after more severe steaming conditions have been applied. The effect will be surpassed when the phosphorus loading becomes very high, when the poisonous effects of acid site loss and reduced accessibility start to dominate again. [33]

5.3 Future Applications

Although hydrocarbon cracking and MTH reactions are the most widely studied reactions for phosphated zeolites, there are also new promising directions where phosphated zeolites can be utilized. An example being the catalytic dehydration of bio-alcohols, such as of ethanol to ethylene. As was discussed in the previous sections, applying a phosphatation step decreases the number and strength of acid-sites in the zeolite, which makes phosphated zeolites very suitable for the selective dehydration of bio-alcohols to alkenes. [63, 77, 81, 83, 84] However, if these reactions are performed in liquid phase the reversible-interactions of phosphorus should be considered (Scheme 4 a). The formation of H_2O during dehydration removes the reversible phosphorus-aluminium interactions, and strong acid sites will reappear, leading to undesired cracking reactions (Scheme 4 b). A possible solution to overcome this problem is to perform a pre-leaching step followed by a post-steam treatment. In this manner, the physical interacting phosphorus is removed and the strong acid sites that form as a consequence can be removed by hydrothermal treatment (Scheme 4 a-d). It is expected that this material has exclusively weak acid sites, which remain weak in aqueous environments.

Another key potential application for phosphated H-ZSM-5 is in catalytic fast pyrolysis of biomass. [2, 12] In this process Ga-ZSM-5 is used to produce high amounts of aromatics from lignocellulosic biomass.[12] However, a major obstacle is the formation of coke during the process, which is resolved by thermal regeneration. Phosphorus stabilization could be a successful method to provide additional stability during the thermal regeneration. A study by Furomoto et al. has shown that phosphorus addition to Ga-ZSM-5 improves stability and suppresses carbonaceous deposits and gallium release from the framework during ethanol-to-propylene reactions.[183] Therefore, we hope to see future studies in the use of phosphorus as a promoter in zeolite catalysed pyrolysis of biomass.

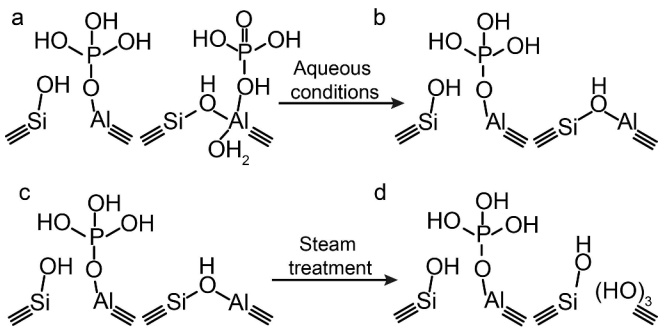

Scheme 4. Schematic representation on the effect of aqueous conditions on permanent and reversible phosphorus-aluminium interactions.

The concepts presented in this review article help the field to modify zeolites by phosphatation more rationally. For example, by exclusive synthesis of local SAPO interfaces in channel intersections of a multi-dimensional 10-MR framework, one obtains a material that has a multi-dimensional framework structure, but not the internal cavities that promote the formation of carbenium ions. In these materials, transport of molecules is still fast, while coke formation and reaction

mechanisms that use carbenium ions are reduced.[181, 182] As the dislodged Si-O-Al-OH species that form during thermal treatment were found to act as anchoring points for phosphoric acid, thermal treatment before phosphatation is a first step in the exclusive formation of local SAPO interfaces. [86]

However, more precise synthesis methods should be explored than the impregnation methods that are often applied to introduce phosphorus. [31, 33-35, 50, 51, 53, 54, 56-60, 63, 64, 66, 68-87, 90-92, 103, 108] As we have read in the previous sections, introduction of phosphoric acid under these conditions leads to inter-, and intra-particle heterogeneities. Gao and co-workers have shown that introduction of phosphorus by means of hydrothermal dispersion leads to a more homogeneous distribution of phosphorus species than by impregnation. [101, 102] Janardhan et al. reported on the formation of phosphate monolayer islands, by performing phosphatation followed by an elution step.[36] The authors argued that the removal of excess phosphorus species is essential for the creation of accessible materials. Although we agree, elution of phosphorus by hot water washing also removes the reversible phosphorus-aluminium interactions. This can be undesirable, as is the case in the dehydration of bio-alcohols. Gas-vapour deposition as a means to introduce phosphorus has been reported to lead to more phosphorus-aluminium interactions, than by wet impregnation. [78] Furthermore, a pre-steam treatment followed by extraction of extra-framework aluminium to form mesopores, could be a method to obtain more efficient transport routes for phosphorus precursors. Extraction of extra-framework aluminium is essential in this step, if the formation of extra-framework $AlPO_4$ is not desired.

Furthermore, if one were to leave the extra-framework aluminium, it is possible to synthesise an aluminium-phosphate binder from the zeolite's own aluminium supply. Especially in the field of catalytic hydrocarbon cracking, the addition of $AlPO_4$ to zeolites, leads to improved light olefin selectivity, hydrothermal stabilization, improved mechanical strength and attrition resistance. [23, 46-48, 184] Furthermore, there are several arguments in favour for creating a binder phase from a zeolite's own aluminium supply. [114] First of all, it allows the use of zeolites with low Si/Al ratios, which are cheaper and more environmentally friendly to produce, as the use of organic templates is not required.[185, 186] Secondly, the formation of mesopores caused by the dealumination step, creates a hierarchical material, facilitating access and transport for reactant and product molecules during catalysis.[187, 188] And finally, careful synthesis of $AlPO_4$ from extra-framework aluminium (EFAl) allows one to form $AlPO_4$ species inside the zeolite channel/cage system, altering its shape selective properties. Although not many studies have been performed in this direction yet, we believe these promising avenues of phosphorus-zeolite chemistry deserve to be investigated.

On a final note, the interaction of phosphorus with zeolites could act as a model system to understand the chemistry between zeolites and other group VA elements, such as arsenic and antimony. Zeolites are very effective materials in removing arsenic from wastewater. [189-191] The suggested condensation reaction of arsenate with the Al-OH groups of surface framework aluminium has certain analogies to that of the formation of local SAPO interfaces. [191] Similar to phosphorus, the modification of H-ZSM-5 with antimony oxide showed increased *para*-selectivity towards toluene disproportionation and a decrease in strong acid sites in H-ZSM-5. [192, 193] As this type of inorganic chemistry has an effect on fields such as biomass conversion, hydrocarbon catalysis, automotive catalysis and wastewater treatment we hope to see future studies that explore and ultimately obtain a unified view of group VA chemistry with zeolite materials.

6. Summary

The study and comparison of the existing literature on phosphorus-zeolite chemistry has revealed many universal physicochemical effects that take place. One of the most important realisations should be that the attraction between phosphorus and aluminium is the driving force behind the physicochemical changes in phosphated zeolites, such as the loss in acid site number, decrease of framework negativity, improved hydrothermal stability and changes in catalytic shape-selectivity. Part of these changes is permanent and caused by SAPO-fication, i.e. the formation of local silico-aluminophosphate (SAPO) interfaces in the zeolite framework. However, a significant other part of these changes can be simply reverted by elution of physically bonded phosphate species. In catalysis the physicochemical changes caused by phosphorous modification can be either promotional or poisonous.

During the phosphorus modification of zeolites by wet impregnation, phosphorus species deposit on the external surface before entering the zeolite channels. Phosphorus enters the zeolite channels with increasing loadings, but diffusion limitations lead to a distribution gradient, with a higher concentration of phosphorus at the outer surface. With weight loadings above 5 wt.% of phosphorus, the formation of large polyphosphates on or near the external surface is observed. Phosphorus species do not cause severe pore blockage at average phosphorus loadings (above 2 wt. %). However, treatment with phosphorus always leads to decreased surface area and micropore volume. This decrease is amplified with increasing phosphorus content.

Excess phosphorus is present as ortho-, pyro-, and polyphosphates. With increasing phosphorus content the amount of excess phosphorus increases. Excess phosphorus dehydrates at high temperatures forming condensed polyphosphates. This effect is reversible. Rehydration leads to the formation of smaller phosphate species. Phosphorus species, that are not interacting with the zeolite framework, can be easily eluted by hot water washing.

Depending on the P/Al ratio and the location of phosphorus, only a certain amount of phosphorus can chemically interact with aluminium in the zeolite. Phosphorus can reversibly interact with tetrahedrally coordinated framework aluminium

(TFAl) species, forcing TFAl species into octahedral coordination. Elution of phosphorus by hot water washing reverses this effect. Phosphorus preferentially reacts with extra-framework aluminium (EFAl) or partially dislodged tetrahedrally coordinated framework aluminium ($TFAl_{dis}$) species. This leads to the formation of (amorphous) extra-framework $AlPO_4$ species and local framework SAPO interfaces. Hot water washing cannot remove these species. Due to the lack of experimental evidence and the unstable character of Si-O-P bonds it seems unlikely that [PO_4] units are fully substituted into the framework to replace [AlO_4] and [SiO_4] tetrahedra.

Introduction of phosphorus leads to the reduction of strong acid sites. This reduction increases with increasing amounts of phosphorus. Phosphorus actively promotes dealumination during thermal treatment. The loss of Si-O-Al bonds and the expected reaction of phosphorus with Si-O-Al-OH species to form neutral local SAPO interfaces leads to permanent loss of Brønsted acid sites. Furthermore, the reversible interactions of phosphorus with framework aluminium before thermal treatment have been shown to lead to a reduction in acid sites as well. At this moment, the exact nature of reversible acid site loss is not understood. The choice of phosphorus precursor does not have a strong influence on the final modification effects after thermal treatment as phosphorus precursors decompose into (poly-) phosphate species.

Besides a reduction in the number of acid sites phosphatation also decreases the average acid site strength. Increasing phosphorus content leads to a further decrease in average acid site strength. There are three causes for the observed decrease in average site strength. (i) A decrease in the acid site strength of bridging hydroxyl groups. (ii) Relative more strong acid sites are decreased by phosphatation than weak acid sites. (iii) An actual increase in the number of weak acid sites. Possible candidates for these new weak acid sites are silanol nests, extra-framework aluminium species and P-OH groups. The question how the average acid site strength is reduced and what the source of new weak acid sites is, asks for more detailed and systematic characterisation studies.

Phosphorus has been shown to have promoting effect on the hydrothermal stability of zeolites H-ZSM-5 and H-IM-5. Relatively more strong acid sites are retained during hydrothermal treatment and the amount of tetrahedrally coordinated framework (TFAl) species that are expelled from the framework are either relatively or absolutely less than in unmodified samples. Like silicoalumino-phosphates, local SAPO interfaces have been found to remain unaffected during steam treatment and since aluminium remains fixed in the framework, the pore structure is better retained. With prolonged steam treatments all Si-O-Al bonds of the SAPO interfaces are hydrolysed, leading to the formation of extra-framework $AlPO_4$. Therefore, we suggest that SAPO interfaces form metastable intermediates during dealumination in the zeolite H-ZSM-5 and H-IM-5 channel system. It is not at all certain if phosphorus has a similar promoting effect on other framework topologies, which should receive more emphasis in further research.

All these physicochemical effects change the activity and selectivity of phosphated zeolites in a range of catalytic applications. In the selective catalytic reduction of NO_x with ammonia over transition metal exchanged zeolites, the presence of phosphorus is extremely deleterious. The breaking of Si-O-Al bonds, leading to reduced framework negativity and acid sites, leads to a decrease in chemisorbed NH_3 and NO_x species. Additionally, the subsequent formation of metal oxides and phosphate species reduces the accessibility of the zeolites even more, leading to severe deactivation.

In catalytic processes to produce hydrocarbons, phosphorus-modified zeolites have generally a higher selectivity towards light olefins, especially propylene, and retain higher activities with time-on-stream compared to their non-phosphated counterparts, due to reduced coke formation and improved hydrothermal stability. The decrease in strong Brønsted acid site number and the increase in weak Brønsted acid sites or weak/strong acid site ratio have most often been attributed as the origin for most performance changes in catalytic reactions such as hydrocarbon cracking, methanol-to-olefins, dehydration of ethanol and alkylation of aromatics. Reactions that demand strong acid sites show a reduced conversion with increasing amounts of phosphorus content. Often, applying higher reaction temperatures increases the overall catalytic conversion. The decrease in acid site number and average acid site strength, leads to a reduction of secondary reactions, such as hydride transfer, cracking and cyclisation reactions. This prevents oligomerization of light olefins, coke formation as well as the cracking of products.

Besides chemical alterations, the introduction of phosphorus into the zeolite channel leads to decreased pore dimensions and reduced accessibility, which in turn lead to longer diffusion pathways for reactants and products. Therefore, products that diffuse fast out of the zeolite will have an improved selectivity. Phosphate species present in the pores act as steric impediments and hinder the formation of bulky (intermediate) products, such as carbenium ions. Therefore, it is suggested that phosphorus modification of H-ZSM-5 inhibits the bimolecular cracking mechanism in alkane cracking and the aromatic-based cycle in methanol-to-hydrocarbon reactions.

Since the post-modification of zeolites with phosphorus is a relative inexpensive way to boost catalyst lifetime and selectivity towards light olefins, and especially since zeolites are important potential players in future sustainable hydrocarbon production processes, it is of high importance to obtain a more fundamental understanding of the underlying physicochemical effects of phosphorus-zeolite chemistry. The universal concepts on phosphorus-zeolite chemistry presented in this review article help the field to modify zeolites by phosphorus more rationally and can act as a frame of reference in future studies to fundamentally understand the interaction of zeolites with group VA elements in general.

Notes and references

[a] Inorganic Chemistry and Catalysis, Faculty of Science, Utrecht University, Universiteitsweg 99, 3584 CG, Utrecht, The Netherlands. E-mail: b.m.weckhuysen@uu.nl Fax: (+31) 30-251-1027

1. U. Olsbye, S. Svelle, M. Bjørgen, P. Beato, T. V. W. Janssens, F. Joensen, S. Bordiga and K. P. Lillerud, *Angew. Chem. Int. Ed.*, 2012, **51**, 5810-5831.
2. G. W. Huber, S. Iborra and A. Corma, *Chem. Rev.*, 2006, **106**, 4044-4098.
3. M. Guisnet and J.-P. Gilson, *Zeolites for cleaner technologies*, Imperial College Press London, 2002.
4. S. Brandenberger, O. Kröcher, A. Tissler and R. Althoff, *Catal. Rev.*, 2008, **50**, 492-531.
5. L. Karwacki, M. H. F. Kox, D. A. Matthijs de Winter, M. R. Drury, J. D. Meeldijk, E. Stavitski, W. Schmidt, M. Mertens, P. Cubillas, N. John, A. Chan, N. Kahn, S. R. Bare, M. Anderson, J. Kornatowski and B. M. Weckhuysen, *Nat. Mater.*, 2009, **8**, 959-965.
6. G. Reding, T. Mäurer and B. Kraushaar-Czarnetzki, *Micropor. Mesopor. Mater.*, 2003, **57**, 83-92.
7. Y. Yan, M. E. Davis and G. R. Gavalas, *Ind. Eng. Chem. Res.*, 1995, **34**, 1652-1661.
8. D. H. Olson, G. T. Kokotailo, S. L. Lawton and W. M. Meier, *J. Phys. Chem.*, 1981, **85**, 2238-2243.
9. www.iza-structure.org.
10. N. Y. Chen, W. W. Kaeding and F. G. Dwyer, *J. Am. Chem. Soc.*, 1979, **101**, 6783-6784.
11. Z. Y. Zakaria, N. A. S. Amin and J. Linnekoski, *Biomass Bioenergy*, 2013, **55**, 370-385.
12. J. Jae, R. Coolman, T. J. Mountziaris and G. W. Huber, *Chem. Eng. Sci.*, 2014, **108**, 33-46.
13. M. Takeuchi, T. Kimura, M. Hidaka, D. Rakhmawaty and M. Anpo, *J. Catal.*, 2007, **246**, 235-240.
14. R. K. Grasselli, D. L. Stern and J. G. Tsikoyiannis, *Appl. Catal. A*, 1999, **189**, 1-8.
15. W. O. Haag, R. M. Lago and P. G. Rodewald, *J. Mol. Catal.*, 1982, **17**, 161-169.
16. L. B. Young, S. A. Butter and W. W. Kaeding, *J. Catal.*, 1982, **76**, 418-432.
17. W. W. Kaeding, C. Chu, L. B. Young, B. Weinstein and S. A. Butter, *J. Catal.*, 1981, **67**, 159-174.
18. C. D. Chang and A. J. Silvestri, *J. Catal.*, 1977, **47**, 249-259.
19. W. R. Moser, R. W. Thompson, C.-C. Chiang and H. Tong, *J. Catal.*, 1989, **117**, 19-32.
20. T. F. Degnan, C. M. Smith and C. R. Venkat, *Appl. Catal. A*, 2001, **221**, 283-294.
21. K. Tanabe and W. F. Hölderich, *Appl. Catal. A*, 1999, **181**, 399-434.
22. H. Mooiweer, K. De Jong, B. Kraushaar-Czarnetzki, W. Stork and B. Krutzen, *Stud. Surrf. Sci. Catal.*, 1994, **84**, 2327-2334.
23. G. Cao, L. R. M. Martens, J. L. White, T. J. Chen and M. J. Shah, US6080303 A, 2000.
24. C. Plank, E. Rosinski and W. Hawthorne, *Ind. Eng. Chem. Prod. Res. Dev.*, 1964, **3**, 165-169.
25. J. E. Otterstedt, S. B. Gevert, S. G. Jääs and P. G. Menon, *Appl. Catal.,* 1986, **22**, 159-179.
26. J. W. Ward, *Fuel Process. Tech.*, 1993, **35**, 55-85.
27. T. F. Degnan, G. K. Chitnis and P. H. Schipper, *Micropor. Mesopor. Mater.*, 2000, **35-36**, 245-252.
28. A. Corma, V. Fornes, W. Kolodziejski and L. J. Martinez-Triguero, *J. Catal.*, 1994, **145**, 27-36.
29. J. C. Védrine, A. Auroux, P. Dejaifve, V. Ducarme, H. Hoser and S. Zhou, *J. Catal.*, 1982, **73**, 147-160.
30. A. F. Costa, H. S. Cerqueira, J. M. M. Ferreira, N. M. S. Ruiz and S. M. C. Menezes, *Appl. Catal. A*, 2007, **319**, 137-143.
31. J. Liu, C. Zhang, Z. Shen, W. Hua, Y. Tang, W. Shen, Y. Yue and H. Xu, *Catal. Commun.*, 2009, **10**, 1506-1509.
32. R. Silver, M. Stefanick and B. Todd, *Catal. Today*, 2008, **136**, 28-33.
33. G. Caeiro, P. Magnoux, J. M. Lopes, F. R. Ribeiro, S. M. C. Menezes, A. F. Costa and H. S. Cerqueira, *Appl. Catal. A*, 2006, **314**, 160-171.
34. T. Blasco, A. Corma and J. Martínez-Triguero, *J. Catal.*, 2006, **237**, 267-277.
35. J. A. Lercher and G. Rumplmayr, *Appl. Catal.,* 1986, **25**, 215-222.
36. H. L. Janardhan, G. V. Shanbhag and A. B. Halgeri, *Appl. Catal. A*, 2014, **471**, 12-18.
37. I. Lezcano-Gonzalez, U. Deka, H. E. van der Bij, P. Paalanen, B. Arstad, B. M. Weckhuysen and A. M. Beale, *Appl. Catal. B*, 2014, **154**, 339-349.
38. A. K. Ghosh, N. Kulkarni and P. L. Harvey, WO2014025371 A1, 2014.
39. D. H. Harris, WO2014042641 A1, 2014.
40. S. Mignard, A. Corma, J. Martinez-Triguero, E. Benazzi, S. Lacombe and G. Mabilon, US6306286 B1, 2001.
41. W. F. Lai, M. A. Hamilton and S. J. Mccarthy, WO2013059176 A1, 2013.
42. M. S. Al-Ghrami and C. Ercan, WO2013177388 A1, 2013.
43. G. Burghels, E. Corresa Mateu, S. Klingelhofer, J. Martinez-Triguero, M. Frauenrath and A. Corma, WO2012123558 A1, 2012.
44. L. A. Chewter, W. J. Van and F. Winter, WO2010133643 A2, 2010.
45. D. L. Johnson, K. E. Nariman and R. A. Ware, WO2001004237 A2, 2001.
46. A. Corma, WO1999002260 A1, 1999.
47. T. G. Roberie and F. T. I. I. John, US5286369 A, 1994.
48. G. W. Kirker, M. E. Landis and J. H. Yen, US4724066 A, 1988.
49. A. J. Tissler and E. T. C. Vogt, WO2001037994 A3, 2001.
50. G. Lischke, R. Eckelt, H. G. Jerschkewitz, B. Parlitz, E. Schreier, W. Storek, B. Zibrowius and G. Öhlmann, *J. Catal.*, 1991, **132**, 229-243.
51. M. J. B. Cardoso, D. D. O. Rosas and L. Y. Lau, *Adsorpt.-J. Int. Adsorpt. Soc.*, 2005, **11**, 577-580.
52. W. W. Kaeding and S. A. Butter, *J. Catal.*, 1980, **61**, 155-164.
53. M. Göhlich, W. Reschetilowski and S. Paasch, *Micropor. Mesopor. Mater.*, 2011, **142**, 178-183.
54. A. Jentys, G. Rumplmayr and J. A. Lercher, *Appl. Catal.,* 1989, **53**, 299-312.
55. K. Damodaran, J. W. Wiench, S. M. Cabral de Menezes, Y. L. Lam, J. Trebosc, J. P. Amoureux and M. Pruski, *Micropor. Mesopor. Mater.*, 2006, **95**, 296-305.
56. J. Caro, M. Bülow, M. Derewinski, J. Haber, M. Hunger, J. Kärger, H. Pfeifer, W. Storek and B. Zibrowius, *J. Catal.*, 1990, **124**, 367-375.
57. N. Xue, X. Chen, L. Nie, X. Guo, W. Ding, Y. Chen, M. Gu and Z. Xie, *J. Catal.*, 2007, **248**, 20-28.

58. J. Zhuang, D. Ma, G. Yang, Z. Yan, X. Liu, X. Liu, X. Han, X. Bao, P. Xie and Z. Liu, *J. Catal.*, 2004, **228**, 234-242.
59. S. M. Abubakar, D. M. Marcus, J. C. Lee, J. O. Ehresmann, C. Y. Chen, P. W. Kletnieks, D. R. Guenther, M. J. Hayman, M. Pavlova, J. B. Nicholas and J. F. Haw, *Langmuir*, 2006, **22**, 4846-4852.
60. A. Yamaguchi, D. Jin, T. Ikeda, K. Sato, N. Hiyoshi, T. Hanaoka, F. Mizukami and M. Shirai, *Catal. Lett.*, 2014, **144**, 44-49.
61. S. M. Campbell, D. M. Bibby, J. M. Coddington and R. F. Howe, *J. Catal.*, 1996, **161**, 350-358.
62. A. T. Aguayo, A. G. Gayubo, A. M. Tarrío, A. Atutxa and J. Bilbao, *J. Chem. Technol. Biotechnol.*, 2002, **77**, 211-216.
63. Z. Song, A. Takahashi, I. Nakamura and T. Fujitani, *Appl. Catal. A*, 2010, **384**, 201-205.
64. G. Zhao, J. Teng, Z. Xie, W. Jin, W. Yang, Q. Chen and Y. Tang, *J. Catal.*, 2007, **248**, 29-37.
65. S. Shwan, J. Jansson, L. Olsson and M. Skoglundh, *Appl. Catal. B*, 2014, **147**, 111-123.
66. L. Lin, C. Qiu, Z. Zhuo, D. Zhang, S. Zhao, H. Wu, Y. Liu and M. He, *J. Catal.*, 2014, **309**, 136-145.
67. M. Derewinski, P. Sarv, X. Sun, S. MÃ¼ller, A. C. Van Veen and J. A. Lercher, *J. Phys. Chem. C*, 2014.
68. K. H. Chandawar, S. B. Kulkarni and P. Ratnasamy, *Appl. Catal.,* 1982, **4**, 287-295.
69. G. Seo and R. Ryoo, *J. Catal.*, 1990, **124**, 224-230.
70. V. N. Romannikov, A. J. Tissler and R. Thome, *React. Kinet. Catal. Lett.*, 1993, **51**, 125-134.
71. S. M. Cabral de Menezes, Y. L. Lam, K. Damodaran and M. Pruski, *Micropor. Mesopor. Mater.*, 2006, **95**, 286-295.
72. M. Ghiaci, A. Abbaspur, M. Arshadi and B. Aghabarari, *Appl. Catal. A*, 2007, **316**, 32-46.
73. M. Ghiaci, A. Abbaspur and R. J. Kalbasi, *Appl. Catal. A*, 2006, **298**, 32-39.
74. R. J. Kalbasi, M. Ghiaci and A. R. Massah, *Appl. Catal. A*, 2009, **353**, 1-8.
75. R. Lü, Z. Cao and X. Liu, *J. Nat. Gas Chem.*, 2008, **17**, 142-148.
76. G. Jiang, L. Zhang, Z. Zhao, X. Zhou, A. Duan, C. Xu and J. Gao, *Appl. Catal. A*, 2008, **340**, 176-182.
77. D. Zhang, R. Wang and X. Yang, *Catal. Lett.*, 2008, **124**, 384-391.
78. Y.-J. Lee, J. M. Kim, J. W. Bae, C.-H. Shin and K.-W. Jun, *Fuel*, 2009, **88**, 1915-1921.
79. N. Xue, L. Nie, D. Fang, X. Guo, J. Shen, W. Ding and Y. Chen, *Appl. Catal. A*, 2009, **352**, 87-94.
80. Z. Wang, G. Jiang, Z. Zhao, X. Feng, A. Duan, J. Liu, C. Xu and J. Gao, *Energy Fuels*, 2009, **24**, 758-763.
81. K. Ramesh, L. M. Hui, Y.-F. Han and A. Borgna, *Catal. Commun.*, 2009, **10**, 567-571.
82. P. Li, W. Zhang, X. Han and X. Bao, *Catal. Lett.*, 2010, **134**, 124-130.
83. N. Zhan, Y. Hu, H. Li, D. Yu, Y. Han and H. Huang, *Catal. Commun.*, 2010, **11**, 633-637.
84. K. Ramesh, C. Jie, Y.-F. Han and A. Borgna, *Ind. Eng. Chem. Res.*, 2011, **49**, 4080-4090.
85. D. Liu, W. C. Choi, C. W. Lee, N. Y. Kang, Y. J. Lee, C.-H. Shin and Y. K. Park, *Catal. Today*, 2011, **164**, 154-157.
86. H. E. van der Bij and B. M. Weckhuysen, *Phys. Chem. Chem. Phys.*, 2014, **16**, 9892-9903.
87. H. E. van der Bij, L. R. Aramburo, B. Arstad, J. J. Dynes, J. Wang and B. M. Weckhuysen, *ChemPhysChem*, 2014, **15**, 283-292.
88. A. Corma, J. Mengual and P. J. Miguel, *Appl. Catal. A*, 2012, **421**, 121-134.
89. M. Dyballa, E. Klemm, J. Weitkamp and M. Hunger, *Chem. Eng. Tech.*, 2013, **85**, 1719-1725.
90. H. Vinek, G. Rumplmayr and J. A. Lercher, *J. Catal.*, 1989, **115**, 291-300.
91. G. Rumplmayr and J. A. Lercher, *Zeolites*, 1990, **10**, 283-287.
92. N. Xue, R. Olindo and J. A. Lercher, *J. Phys. Chem. C*, 2010, **114**, 15763-15770.
93. W. W. Kaeding, C. Chu, L. B. Young and S. A. Butter, *J. Catal.*, 1981, **69**, 392-398.
94. P. Tynjälä, T. T. Pakkanen and S. Mustamaki, *J. Phys. Chem. B*, 1998, **102**, 5280-5286.
95. J. Nunan, J. Cronin and J. Cunningham, *J. Catal.*, 1984, **87**, 77-85.
96. A. Rahman, G. Lemay, A. Adnot and S. Kaliaguine, *J. Catal.*, 1988, **112**, 453-463.
97. A. Rahman, A. Adnot, G. Lemay, S. Kaliaguine and G. Jean, *Appl. Catal.,* 1989, **50**, 131-147.
98. M. Kojima, F. Lefebvre and Y. Ben Taârit, *Zeolites*, 1992, **12**, 724-727.
99. W. Reschetilowski, B. Meier, M. Hunger, B. Unger and K. P. Wendlandt, *Angew. Chem. Int. Ed.*, 1991, **30**, 686-687.
100. B. Viswanathan and A. C. Pulikottil, *Catal. Lett.*, 1993, **22**, 373-379.
101. X. Gao, Z. Tang, D. Ji and H. Zhang, *Catal. Commun.*, 2009, **10**, 1787-1790.
102. X. Gao, Z. Tang, H. Zhang, C. Liu, Z. Zhang, G. Lu and D. Ji, *Kor. J. Chem. Eng.*, 2010, **27**, 812-815.
103. M. Derewinski, P. Sarv, X. Sun, S. Müller, A. C. van Veen and J. A. Lercher, *J. Phys. Chem. C*, 2014, **118**, 6122-6131.
104. Y. Huang, X. Dong, M. Li, M. Zhang and Y. Yu, *RSC Adv.*, 2014, **4**, 14573-14581.
105. T. Fjermestad, S. Svelle and O. Swang, *J. Phys. Chem. C*, 2013, **117**, 13442-13451.
106. S. Malola, S. Svelle, F. L. Bleken and O. Swang, *Angew. Chem. Int. Ed.*, 2012, **51**, 652-655.
107. S. M. Campbell, D. M. Bibby, J. M. Coddington, R. F. Howe and R. H. Meinhold, *J. Catal.*, 1996, **161**, 338-349.
108. H. E. van der Bij, F. Meirer, S. Kalirai, J. Wang and B. M. Weckhuysen, *Chem. Eur. J.*, 2014, **20**, 16922-16932.
109. S. M. Bradley and R. F. Howe, *Micropor. Mater.*, 1997, **12**, 13-19.
110. Z. Liu, Z.-X. Chen, W. Ding, G.-J. Kang and Z. Li, *J. Mol. Struc.-THEOCHEM*, 2010, **948**, 99-101.
111. P. H. Zeng, Y. Liang, S. F. Ji, B. J. Shen, H. H. Liu, B. J. Wang, H. J. Zhao and M. F. Li, *J. Energy Chem.*, 2014, **23**, 193-200.
112. M. Hunger, Wiley-VCH: Weinheim, 2010, vol. 2, pp. 493-546.
113. X. Wang, W. Dai, G. Wu, L. Li, N. Guan and M. Hunger, *Micropor. Mesopor. Mater.*, 2012, **151**, 99-106.
114. H. E. Van der Bij, D. Cicmil, J. Wang, F. Meirer, F. M. F. de Groot and B. M. Weckhuysen, *J. Am. Chem. Soc.*, 2014, **136**, 17774-17787.
115. E. W. Shin, J. S. Han, M. Jang, S.-H. Min, J. K. Park and R. M. Rowell, *Environ. Sci. Tech.*, 2003, **38**, 912-917.
116. J. W. Wiench, G. Tricot, L. Delevoye, J. Trebosc, J. Frye, L. Montagne, J.-P. Amoureux and M. Pruski, *Phys. Chem. Chem. Phys.*, 2006, **8**, 144-150.

117. Y. Wang, B. Shen, L. Wang, B. Feng, J. Li and Q. Guo, *Fuel Process. Tech.*, 2013, **106**, 141-148.
118. M. Müller, G. Harvey and R. Prins, *Micropor. Mesopor. Mater.*, 2000, **34**, 135-147.
119. G. Sastre, D. W. Lewis and C. R. A. Catlow, *J. Phys. Chem.*, 1996, **100**, 6722-6730.
120. D. Barthomeuf, *Zeolites*, 1994, **14**, 394-401.
121. J. Tan, Z. Liu, X. Bao, X. Liu, X. Han, C. He and R. Zhai, *Micropor. Mesopor. Mater.*, 2002, **53**, 97-108.
122. S. L. Suib, A. M. Winiecki and A. Kostapapas, *Langmuir*, 1987, **3**, 483-488.
123. R. Lü, Z. Cao and S. Wang, *J. Mol. Struc.-THEOCHEM*, 2008, **865**, 1-7.
124. R. M. Barrer and M. Liquornik, *J. Chem. Soc., Dalton Trans.*, 1974, 2126-2128.
125. N. J. Clayden, S. Esposito, P. Pernice and A. Aronne, *J. Mater. Chem.*, 2001, **11**, 936-943.
126. C. Coelho, T. Azaïs, L. Bonhomme-Coury, G. Laurent and C. Bonhomme, *Inorg. Chem.*, 2007, **46**, 1379-1387.
127. G. H. Kühl and K. D. Schmitt, *Zeolites*, 1990, **10**, 2-7.
128. A. Corma, J. Mengual and P. J. Miguel, *Appl. Catal. A*, 2013, **460–461**, 106-115.
129. Q. Cui, Y. Zhou, Q. Wei, G. Yu and L. Zhu, *Fuel Process. Tech.*, 2013, **106**, 439-446.
130. Y. Wang, B. Shen, K. Hao, J. Li, L. Wang, B. Feng and Q. Guo, *Catal. Commun.*, 2012, **25**, 59-63.
131. E. Loeffler, U. Lohse, C. Peuker, G. Oehlmann, L. M. Kustov, V. L. Zholobenko and V. B. Kazansky, *Zeolites*, 1990, **10**, 266-271.
132. J. A. van Bokhoven, A. M. J. van der Eerden and D. C. Koningsberger, *J. Am. Chem. Soc.*, 2003, **125**, 7435-7442.
133. B. Zhao, H. Pan and J. H. Lunsford, *Langmuir*, 1999, **15**, 2761-2765.
134. C. Liu, X. Gao, Z. Zhang, H. Zhang, S. Sun and Y. Deng, *Appl. Catal. A*, 2004, **264**, 225-228.
135. P. Tynjälä and T. T. Pakkanen, *Micropor. Mesopor. Mater.*, 1998, **20**, 363-369.
136. J. Gopalakrishnan, *Chem. Mater.*, 1995, **7**, 1265-1275.
137. S. van Donk, A. H. Janssen, J. H. Bitter and K. P. de Jong, *Catal. Rev.*, 2003, **45**, 297-319.
138. M.-C. Silaghi, C. Chizallet and P. Raybaud, *Micropor. Mesopor. Mater.*, 2014, **191**, 82-96.
139. O. Lisboa, M. Sánchez and F. Ruette, *J. Mol. Catal. A*, 2008, **294**, 93-101.
140. T. Chevreau, A. Chambellan, J. Lavalley, E. Catherine, M. Marzin, A. Janin, J. Hemidy and S. Khabtou, *Zeolites*, 1990, **10**, 226-234.
141. C. S. Triantafillidis, A. G. Vlessidis, L. Nalbandian and N. P. Evmiridis, *Micropor. Mesopor. Mater.*, 2001, **47**, 369-388.
142. T.-H. Chen, K. Houthoofd and P. J. Grobet, *Micropor. Mesopor. Mater.*, 2005, **86**, 31-37.
143. J. Jiao, J. Kanellopoulos, W. Wang, S. S. Ray, H. Foerster, D. Freude and M. Hunger, *Phys. Chem. Chem. Phys.*, 2005, **7**, 3221-3226.
144. Z. Yu, S. Li, Q. Wang, A. Zheng, X. Jun, L. Chen and F. Deng, *J. Phys. Chem. C*, 2011, **115**, 22320-22327.
145. I. Wang, T.-J. Chen, K.-J. Chao and T.-C. Tsai, *J. Catal.*, 1979, **60**, 140-147.
146. L. R. Aramburo, E. de Smit, B. Arstad, M. M. van Schooneveld, L. Sommer, A. Juhin, T. Yokosawa, H. W. Zandbergen, U. Olsbye, F. M. F. de Groot and B. M. Weckhuysen, *Angew. Chem. Int. Ed.*, 2012, **51**, 3616-3619.
147. S. M. T. Almutairi, B. Mezari, E. A. Pidko, P. C. M. M. Magusin and E. J. M. Hensen, *J. Catal.*, 2013, **307**, 194-203.
148. A. Corma, M. Faraldos and A. Mifsud, *Appl. Catal.,* 1989, **47**, 125-133.
149. G. T. Kerr, *J. Phys. Chem.*, 1967, **71**, 4155-4156.
150. C. S. Cundy and P. A. Cox, *Chem. Rev.*, 2003, **103**, 663-702.
151. R. Ryoo and S. Jun, *J. Phys. Chem. B*, 1997, **101**, 317-320.
152. L. R. Aramburo, Y. Liu, T. Tyliszczak, F. M. F. de Groot, J. C. Andrews and B. M. Weckhuysen, *ChemPhysChem*, 2013, **14**, 496-499.
153. L. R. Aramburo, L. Karwacki, P. Cubillas, S. Asahina, D. A. M. de Winter, M. R. Drury, I. L. C. Buurmans, E. Stavitski, D. Mores, M. Daturi, P. Bazin, P. Dumas, F. Thibault-Starzyk, J. A. Post, M. W. Anderson, O. Terasaki and B. M. Weckhuysen, *Chem. Eur. J.*, 2011, **17**, 13773-13781.
154. J. Jiao, S. Altwasser, W. Wang, J. Weitkamp and M. Hunger, *J. Phys. Chem. B*, 2004, **108**, 14305-14310.
155. M. Briend, A. Shikholeslami, M.-J. Peltre, D. Delafosse and D. Barthomeuf, *J. Chem. Soc., Dalton Trans.*, 1989, 1361-1362.
156. S. Wilson and P. Barger, *Micropor. Mesopor. Mater.*, 1999, **29**, 117-126.
157. J. P. Lourenço, M. F. Ribeiro, F. R. Ribeiro, J. Rocha, Z. Gabelica and E. G. Derouane, *Micropor. Mater.*, 1995, **4**, 445-453.
158. L. Huang and Q. Li, *Chem. Lett.*, 1999, **28**, 829-830.
159. M. Bjørgen, F. Joensen, M. Spangsberg Holm, U. Olsbye, K.-P. Lillerud and S. Svelle, *Appl. Catal. A*, 2008, **345**, 43-50.
160. U. Deka, I. Lezcano-Gonzalez, B. M. Weckhuysen and A. M. Beale, *ACS Catal.*, 2013, **3**, 413-427.
161. M. Devadas, O. Kröcher, M. Elsener, A. Wokaun, G. Mitrikas, N. Söger, M. Pfeifer, Y. Demel and L. Mussmann, *Catal. Today*, 2007, **119**, 137-144.
162. P. Kern, M. Klimczak, T. Heinzelmann, M. Lucas and P. Claus, *Appl. Catal. B*, 2010, **95**, 48-56.
163. S. Kotrel, H. Knözinger and B. C. Gates, *Micropor. Mesopor. Mater.*, 2000, **35–36**, 11-20.
164 A. Corma and A. V. Orchillés, *Micropor. Mesopor. Mater.*, 2000, **35–36**, 21-30.
165. C. B. Phillips and R. Datta, *Ind. Eng. Chem. Res.*, 1997, **36**, 4466-4475.
166. W. Dai, X. Wang, G. Wu, L. Li, N. Guan and M. Hunger, *ChemCatChem*, 2012, **4**, 1428-1435.
167. C. D. Chang, C. T. W. Chu and R. F. Socha, *J. Catal.*, 1984, **86**, 289-296.
168. C. Mei, P. Wen, Z. Liu, H. Liu, Y. Wang, W. Yang, Z. Xie, W. Hua and Z. Gao, *J. Catal.*, 2008, **258**, 243-249.
169. F. L. Bleken, S. Chavan, U. Olsbye, M. Boltz, F. Ocampo and B. Louis, *Appl. Catal. A*, 2012, **447–448**, 178-185.
170. A. F. H. Wielers, M. Vaarkamp and M. F. M. Post, *J. Catal.*, 1991, **127**, 51-66.
171. B. S. Greensfelder, H. H. Voge and G. M. Good, *Ind. Eng. Chem.*, 1949, **41**, 2573-2584.
172. N. Rahimi and R. Karimzadeh, *Appl. Catal. A*, 2011, **398**, 1-17.

173. F. C. Jentoft and B. C. Gates, *Top. Catal.*, 1997, **4**, 1-13.
174. K. Kubo, H. Iida, S. Namba and A. Igarashi, *Micropor. Mesopor. Mater.*, 2014, **188**, 23-29.
175. F. Bleken, M. BjÃ¸rgen, L. Palumbo, S. Bordiga, S. Svelle, K.-P. Lillerud and U. Olsbye, *Top. Catal.*, 2009, **52**, 218-228.
176. A. Takahashi, W. Xia, I. Nakamura, H. Shimada and T. Fujitani, *Appl. Catal. A*, 2012, **423**, 162-167.
177. S. Teketel, S. Svelle, K.-P. Lillerud and U. Olsbye, *ChemCatChem*, 2009, **1**, 78-81.
178. F. Bager, N. L. Salas and S. Ernst, *Oil Gas-Eur. Mag.*, 2012, **38**, 107-111.
179. R. Bastiani, Y. L. Lam, C. A. Henriques and V. Teixeira da Silva, *Fuel*, 2013, **107**, 680-687.
180. O. Bortnovsky, P. Sazama and B. Wichterlova, *Appl. Catal. A*, 2005, **287**, 203-213.
181. D. Mores, E. Stavitski, M. H. F. Kox, J. Kornatowski, U. Olsbye and B. M. Weckhuysen, *Chem. Eur. J.*, 2008, **14**, 11320-11327.
182. M. J. Wulfers and F. C. Jentoft, *J. Catal.*, 2013, **307**, 204-213.
183. Y. Furumoto, Y. Harada, N. Tsunoji, A. Takahashi, T. Fujitani, Y. Ide, M. Sadakane and T. Sano, *Appl. Catal. A*, 2011, **399**, 262-267.
184. Y.-J. Lee, Y.-W. Kim, N. Viswanadham, K.-W. Jun and J. W. Bae, *Appl. Catal. A*, 2010, **374**, 18-25.
185. G. Majano, L. Delmotte, V. Valtchev and S. Mintova, *Chem. Mater.*, 2009, **21**, 4184-4191.
186. F. J. Machado, C. M. López, M. a. A. Centeno and C. Urbina, *Appl. Catal. A*, 1999, **181**, 29-38.
187. M. Hartmann, *Angew. Chem. Int. Ed.*, 2004, **43**, 5880-5882.
188. J. Perez-Ramirez, C. H. Christensen, K. Egeblad, C. H. Christensen and J. C. Groen, *Chem. Soc. Rev.*, 2008, **37**, 2530-2542.
189. Y. Xu, T. Nakajima and A. Ohki, *J. Hazard. Mater.*, 2002, **92**, 275-287.
190. S. Shevade and R. G. Ford, *Water Res.*, 2004, **38**, 3197-3204.
191. P. Chutia, S. Kato, T. Kojima and S. Satokawa, *J. Hazard. Mater.*, 2009, **162**, 440-447.
192. D. Mao, J. Xia, B. Zhang and G. Lu, *Energy Convers. Manage.*, 2010, **51**, 1134-1139.
193. S. Zheng, A. Jentys and J. A. Lercher, *J. Catal.*, 2003, **219**, 310-319.